

Hydrogen Separation Membranes

Annual Report for FY 2008

Energy Systems Division

About Argonne National Laboratory

Argonne is a U.S. Department of Energy laboratory managed by UChicago Argonne, LLC under contract DE-AC02-06CH11357. The Laboratory's main facility is outside Chicago, at 9700 South Cass Avenue, Argonne, Illinois 60439. For information about Argonne and its pioneering science and technology programs, see www.anl.gov.

Availability of This Report

This report is available, at no cost, at <http://www.osti.gov/bridge>. It is also available on paper to the U.S. Department of Energy and its contractors, for a processing fee, from:

U.S. Department of Energy
Office of Scientific and Technical Information
P.O. Box 62
Oak Ridge, TN 37831-0062
phone (865) 576-8401
fax (865) 576-5728
reports@adonis.osti.gov

Disclaimer

This report was prepared as an account of work sponsored by an agency of the United States Government. Neither the United States Government nor any agency thereof, nor UChicago Argonne, LLC, nor any of their employees or officers, makes any warranty, express or implied, or assumes any legal liability or responsibility for the accuracy, completeness, or usefulness of any information, apparatus, product, or process disclosed, or represents that its use would not infringe privately owned rights. Reference herein to any specific commercial product, process, or service by trade name, trademark, manufacturer, or otherwise, does not necessarily constitute or imply its endorsement, recommendation, or favoring by the United States Government or any agency thereof. The views and opinions of document authors expressed herein do not necessarily state or reflect those of the United States Government or any agency thereof, Argonne National Laboratory, or UChicago Argonne, LLC.

Hydrogen Separations Membranes

Annual Report for FY 2008

by
U. (Balu) Balachandran, S.E. Dorris, J.E. Emerson, T.H. Lee, Y. Lu, C.Y. Park, and J.J. Picciolo
Energy Systems Division, Argonne National Laboratory

February 11, 2009

**HYDROGEN SEPARATION MEMBRANES
ANNUAL REPORT FOR FY 2008**

ARGONNE NATIONAL LABORATORY

Energy Systems Division

9700 South Cass Avenue

Argonne, Illinois 60439

U. (Balu) Balachandran

Contributors:

S. E. Dorris

Y. Lu

J. E. Emerson

C.Y. Park

T. H. Lee

J. J. Picciolo

January 28, 2009

Work Supported by

U. S. DEPARTMENT OF ENERGY

Office of Fossil Energy, National Energy Technology Laboratory

Argonne National Laboratory is a U.S. Department of Energy laboratory managed by UChicago Argonne, LLC, under Contract Number DE-AC-02-06CH11357.

Contents

I. Objective.....	1
II. Highlights.....	1
III. Introduction.....	2
IV. Results.....	3
Milestone 1. Fabricate tubular membrane.	3
Milestone 2. Test tubular membrane in syngas atmospheres..	8
Milestone 3. Correlate stability phase boundary data with hydrogen flux measurements.....	13
Additional. Effect of Sintering Aids on Microstructure of Thin Film HTMs.....	23
V. Future Work.....	25
VI. Publications and Presentations.....	26
References.....	33

Figures

1. Porous alumina tube coated with ANL-3 film on spring-loaded fixture used to measure its hydrogen flux	4
2. Hydrogen flux of tubular HTM thin films made of Pd/ZrO ₂ or Pd/CeO ₂ , normalized to thickness of 30 μm	5
3. Hydrogen permeability of tubular Pd/ZrO ₂ and Pd/CeO ₂ HTM thin films	5
4. Flow rate of hydrogen through Pd (60 vol.)/TZ-3Y film on porous Al ₂ O ₃ tube measured with various gas flow rates (ml/min).....	6
5. Hydrogen flux of tubular ANL-3e thin film at 725°C, measured using feed gas with various composition and N ₂ as sweep gas.	9
6. Sample holder with ANL-3e tube showing coke that developed during hydrogen flux measurements at 725°C in feed gas with various composition	11
7. Hydrogen flux of ANL-3e thin film (thickness ≈18 μm) measured using N ₂ as sweep gas and 90% H ₂ /balance He as feed gas.	13
8. Hydrogen flux of ANL-3e membrane #1 (thickness ≈250 μm) at ≈725°C in feed gas with ≈10% H ₂ (fixed) and ≈0-400 ppm H ₂ S	15
9. Micrographs of membrane used to collect data in Fig. 8: a) cross-section of Pd ₄ S layer on membrane's surface, and b) top view of Pd ₄ S layer.....	16
10. Hydrogen flux of ANL-3e membrane #2 (thickness ≈330 μm) at ≈725°C in feed gas with ≈10% H ₂ (fixed) and ≈0-155 ppm H ₂ S	17
11. Pd/Pd ₄ S phase boundary determined at Argonne.....	17
12. Hydrogen flux for Pd foil #1 (thickness ≈100 μm) at ≈725°C in feed gas with constant H ₂ concentration (≈10%) and ≈0-155 ppm H ₂ S.....	18
13. Hydrogen flux for Pd foil #2 (thickness ≈100 μm) at ≈725°C in feed gas with constant H ₂ concentration (≈10%) and ≈0-100 ppm H ₂ S.....	19
14. Hydrogen flux for Pd foil #3 (thickness ≈100 μm) at ≈725°C in feed gas with constant H ₂ concentration (≈10%) and ≈0-100 ppm H ₂ S.....	20
15. Percentage of hydrogen in sweep gas attributed to leakage during flux measurements with Pd foil #3 (thickness ≈100 μm) at 725°C in feed gas with constant H ₂ concentration (≈10%) and ≈0-100 ppm H ₂ S.....	20
16. Micrographs of Pd foil #3 (thickness ≈100 μm) before and after its flux was measured at 725°C in feed gas with 10% H ₂ and ≈0-100 ppm H ₂ S.....	21

17. Hydrogen flux of ANL-3e membrane #3 (thickness $\approx 150 \mu\text{m}$) at 725°C in feed gas with constant H_2 concentration ($\approx 10\%$) and $\approx 0\text{-}100 \text{ ppm H}_2\text{S}$	22
18. Micrographs of ANL-3e membrane #3 (thickness $\approx 150 \mu\text{m}$) before and after flux was measured at 725°C in feed gas with $10\% \text{ H}_2$ and $\approx 0\text{-}100 \text{ ppm H}_2\text{S}$	22
19. Micrographs of Pd/ZrO ₂ films on porous alumina with various additives that were tested as possible sintering aids	24

Tables

1. Effect of feed and sweep gas flow rates on hydrogen flux of tubular ANL-3e thin film membrane	12
2. Effect of various additives on porosity of Pd(60 vol. %)/ZrO ₂ thin films on porous Al ₂ O ₃ disks sintered at 1400°C for 5 h in air, compared to "base" film, i.e. film made with no additive	25

HYDROGEN SEPARATION MEMBRANES -- ANNUAL REPORT FOR FY 2008
ARGONNE NATIONAL LABORATORY

Project Title: Development of Dense Ceramic Membranes for Hydrogen Separation

NETL Project Manager: Richard Dunst

ANL Project PI: U. (Balu) Balachandran

B&R Code/Contract Number: AA-10-40-00-0 & AA-20-15-00-0/FWP 49601

Report Date: January 28, 2009

I. OBJECTIVE

The objective of this work is to develop dense ceramic membranes for separating hydrogen from other gaseous components in a nongalvanic mode, i.e., without using an external power supply or electrical circuitry.

II. HIGHLIGHTS

1. A thin-film membrane (ANL-3) on a porous support gave the highest hydrogen flux (≈ 26 and ≈ 50 $\text{cm}^3/\text{min}\cdot\text{cm}^2$ at 400 and 900°C, respectively) to date for Argonne membranes tested under ambient pressure.

2. Two types of ANL-3 thin-film membranes were fabricated on porous alumina support tubes: Pd(60 vol.+)/ZrO₂ and Pd(60 vol.+)/CeO₂.

3. A tubular thin-film membrane (≈ 8 cm long x ≈ 1 cm O.D. x ≈ 60 μm thick) composed of Pd(60 vol.+)/ZrO₂ passed hydrogen at a rate of up to ≈ 190 cm^3 (STP)/min under ambient pressure.

4. A tubular ANL-3e membrane was tested in simulated "syngas" composed of 50.0 mol.% H₂, 23.4% CO, 0.75% CO₂, balance He with and without 50 ppm H₂S.

5. Hydrogen flux measurements for ANL-3e membranes (60 vol.% Pd/ZrO₂) and commercial Pd foils were correlated with Pd/Pd₄S phase boundary data measured in experiments at Argonne.

6. For either ANL-3e or Pd foil samples, H₂S affected hydrogen flux minimally if Pd₄S did not form, but ANL-3e and Pd foil samples appeared to behave differently when Pd₄S formed.

7. The test fixture and reactor for high pressure measurements were modified to measure hydrogen flux according to the test protocol developed at National Energy Technology Laboratory during a project status review meeting.

III. INTRODUCTION

The goal of this project is to develop dense hydrogen transport membranes (HTMs) that nongalvanically (i.e., without electrodes or external power supply) separate hydrogen from gas mixtures at commercially significant fluxes under industrially relevant operating conditions. HTMs will be used to separate hydrogen from gas mixtures such as the product streams from coal gasification, methane partial oxidation, and water-gas shift reactions. Potential ancillary uses of HTMs include dehydrogenation and olefin production, as well as hydrogen recovery in petroleum refineries and ammonia synthesis plants, the largest current users of deliberately produced hydrogen. This report describes progress that was made during FY 2008 on the development of HTM materials.

Materials development for the HTM follows a three-pronged approach at Argonne. In one approach, we utilize principles of solid-state defect chemistry to properly dope selected monolithic electronic/protonic conductors (perovskites doped on both A- and B-sites) and to obtain materials that are chemically stable and have suitable protonic and electronic conductivities. The second approach uses cermet (i.e., ceramic/metal composite) membranes that are prepared by homogeneously mixing electronic/protonic conductors with a metallic component. The metal phase in these cermets enhances the hydrogen permeability of the ceramic phase by increasing the electronic conductivity and by providing an additional transport path for the hydrogen if the metal has high hydrogen permeability. In our third approach, we disperse a metal with high hydrogen permeability (called a "hydrogen transport metal") in a support matrix composed of either a ceramic or a metal. In these composites, hydrogen is transported almost exclusively through the hydrogen transport metal, and the matrix serves primarily as a chemically stable structural support. Our focus during FY 2008 was on the development of HTMs in which a ceramic phase provided structural support for a hydrogen transport metal. In particular, we focused on ANL-3e membranes (composed of Pd mixed with Y_2O_3 -stabilized ZrO_2), which have given the highest hydrogen flux to date for membranes made at Argonne (≈ 26 and ≈ 50 $cm^3/min\text{-}cm^2$ at 400 and 900°C, respectively). Various membranes developed at Argonne are summarized elsewhere. [1]

Good chemical stability is a critical requirement for HTMs due to the corrosiveness of product streams from coal gasification and/or methane reforming. A particularly corrosive contaminant that HTMs might encounter is hydrogen sulfide (H_2S), which can react with Pd-containing HTMs to form Pd_4S . Because Pd_4S impedes hydrogen permeation, we identified conditions under which ANL-3e membranes form Pd_4S [2]. The Pd/ Pd_4S phase boundary was determined for feed gas with 10% and 73% H_2 , because the hydrogen concentration affects the phase boundary's position. To correlate the phase boundary data with the effects of H_2S on the performance of Pd-containing HTMs, we measured the hydrogen flux for commercial Pd foils and ANL-3e membranes that were exposed to feed gas with a fixed hydrogen concentration ($\approx 10\%$) while the H_2S concentration was gradually increased. We tested the chemical stability of a tubular ANL-3e membrane by monitoring the hydrogen flux during its exposure to simulated syngas. Results from these experiments are presented in this report.

In addition to providing high hydrogen flux and being chemically stable, practical HTMs must be available in shapes with a large active area (e.g., tubes). To fabricate tubular HTMs, we adapted the paste-painting method used to prepare a disk-shaped membrane that gave the record high hydrogen flux for Argonne membranes [3]. In the paste-painting approach, porous alumina tubes are first produced by cold isostatic pressing of alumina hydrate powder. After pre-sintering, the tube is painted with a slurry of HTM components and sintered at high temperature to produce a porous tube coated with a dense, thin (25-50 μm) film membrane. By this method, we made tubular thin-film membranes composed of either Pd (60 vol.+)/ZrO₂ [2] or Pd (60 vol.+)/CeO₂ [4]. In this report, we compare the properties of tubes made with the two types of HTM films.

Hydrogen transport membranes must also have good mechanical integrity at high temperature ($\approx 900^\circ\text{C}$) and high pressure (≈ 350 psi). Argonne HTMs have been tested in high-pressure tests at the National Energy Technology Laboratory (NETL) [1] and at Argonne. In tests using Argonne's high-pressure reactor, the hydrogen flux of disk-shaped, self-supported ANL-3e samples was measured in feed gas that contained either 4% H₂ or 90% H₂ at temperatures up to 900°C and pressures up to ≈ 300 psig [2]. The reactor has since been modified to allow thin-film HTMs (thickness ≈ 25 -50 μm) on porous supports to be tested according to criteria established at NETL. To aid in the development of HTMs that satisfy the requirements described above, the following milestones were established in the Field Work Proposal for FY 2008:

1. Fabricate tubular membrane.
2. Test tubular membrane in syngas atmospheres.
3. Correlate stability phase boundary data with hydrogen flux measurements.

All experimental milestones for FY 2008 were met using membranes that were developed at Argonne. In addition to meeting these milestones, we continued developing new membrane materials and fabrication methods to increase the hydrogen flux of HTMs.

IV. RESULTS

Results obtained during FY 2008 are presented below in relation to the pertinent milestone. Also described is work that was done outside the scope of the milestones.

Milestone 1. Fabricate tubular membrane.

Porous support tubes (one end closed) for making tubular thin-film membranes were pressed at 10,000-15,000 psig in a cold isostatic press (Engineered Pressure Systems, Inc.) using alumina hydrate powder and a rubber mold (Trexler Rubber) with a stainless steel mandrel. After being pressed, the support tube was pre-sintered for 3-5 h at 800-950°C in air. The tube's outer surface was painted with a slurry of ANL-3 components [either CeO₂ or TZ-3Y (ZrO₂ partially stabilized by Y₂O₃) mixed with Pd powder (60 vol.)], and the painted tube was sintered for 5 h at 1400-1500°C in air. Typical dimensions for tubular membranes are ≈ 30 -60 μm (thickness of thin film membrane) x ≈ 8 cm (length) x ≈ 1 cm (outside diameter).

Tubular thin films were tested for pinholes and/or microcracks by checking for penetration of the film by isopropyl alcohol (IPA). In this test, the tube was filled with IPA and examined for evidence that IPA penetrated the film on its outer surface. Penetration of the film by even a small amount of IPA was visible as a darkening of the surface, indicating that the membrane film contained cracks or interconnected porosity.

If an IPA-test revealed no leakage, we measured a tube's hydrogen flux using a spring-loaded test fixture (Fig. 1). Spring-loaded alumina rods squeezed graphite gaskets between the membrane tube and an alumina plate (at right of membrane in Fig. 1) and an alumina tube (on the left in Fig. 1). Placing the end of the membrane tube into a rounded ceramic cup improved alignment between the membrane and the alumina tube, thereby improving the seal. Sweep gas was passed through the inside of the tubular membrane through a small alumina tube (not shown in Fig. 1). To achieve a leak-tight seal, the open ends of the tube were polished so that they were flat and perpendicular to the axis of the tube. When the pre-sintered support tube was coated with membrane material, paste for making the membrane was painted onto the outer surface of the support tube, including the open end, to improve the seal at the ends of the tube.

A tube was heated to 500°C while He was flowed on its feed side and N₂ on its sweep side. The hydrogen flux and permeability were measured with a sweep gas of N₂ and a feed gas of 90% H₂/balance He (both flowing at 150-500 ml/min). The H₂ and He concentrations were measured with a Hewlett-Packard 6890 gas chromatograph. The measured He concentration was used to correct the H₂ concentration for leakage.

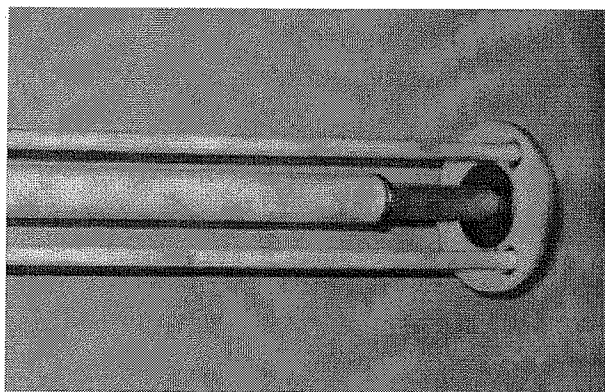


Fig. 1 Porous alumina tube coated with ANL-3 film mounted on spring-loaded fixture used to measure its hydrogen flux.

Figure 2 compares the hydrogen flux values for two tubular thin films, one composed of Pd(60 vol.)/TZ-3Y, the other Pd(60 vol.)/CeO₂. The thickness of the Pd/TZ-3Y film was 58(±4) μm, and that of the Pd/CeO₂ film was 30 μm. To directly compare flux values for the tubes, we multiplied the actual flux values for the Pd/TZ-3Y tube by a factor of 58 μm/30 μm. The flux values (Fig. 2) were measured at feed- and sweep-gas flow rates of 150 ml/min. Figure 3 plots the hydrogen permeability for the tubes. The total hydrogen flow rate through the Pd/TZ-3Y tube (surface area of 23.6 cm²) was calculated and is plotted versus temperature in Fig. 4.

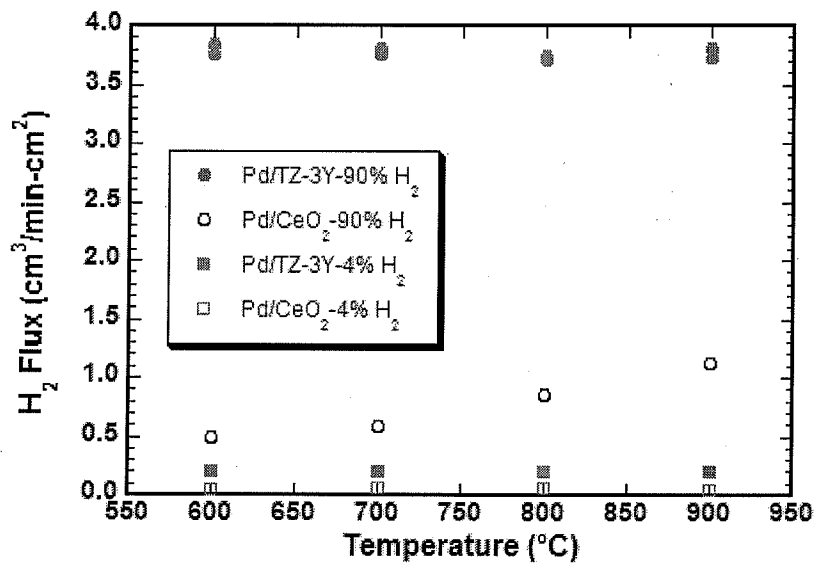


Fig. 2 Hydrogen flux of tubular HTM thin films made of Pd/TZ-3Y and Pd/CeO₂, normalized to thickness of 30 μm. Inset gives feed gas composition.

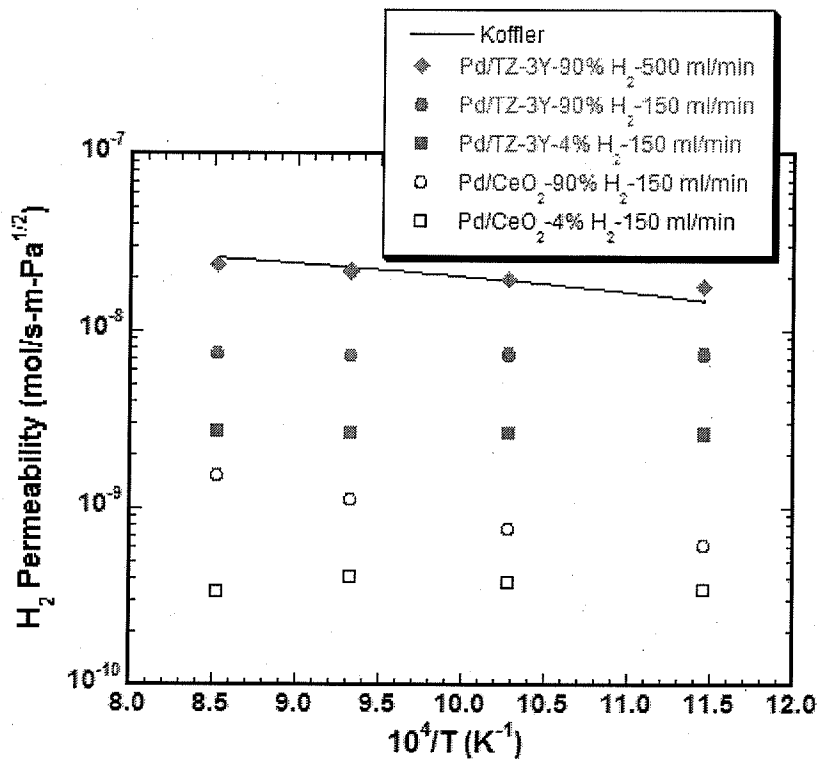


Fig. 3 Hydrogen permeability of tubular HTM thin films composed of Pd/TZ-3Y and Pd/CeO₂. Inset gives composition and flow rate of feed gas.

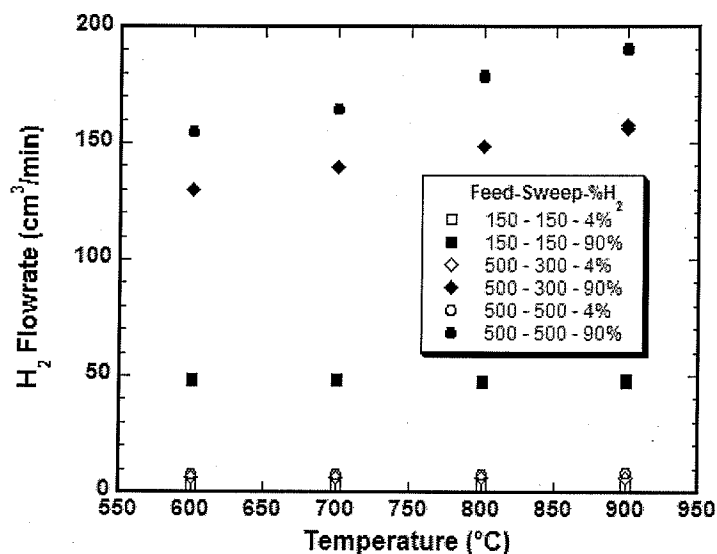


Fig. 4 Flow rate of H_2 through 58- μm -thick Pd (60 vol.%) / TZ-3Y film on porous Al_2O_3 tube measured with various gas flow rates (ml/min). Inset gives feed flow rate, sweep flow rate, and H_2 concentration (%) in feed gas. Sweep gas was 100% N_2 .

With the same feed gas, the flux (Fig. 2) and permeability (Fig. 3) values were lower for the Pd/CeO₂ tube than for the Pd/TZ-3Y tube, especially when the feed gas was 90% H_2 /balance He. Several factors might contribute to the inferior performance of the Pd/CeO₂ tube. First, Pd/CeO₂ films tend to attain higher density during sintering than do Pd/TZ-3Y films. The higher density decreases the likelihood of leaks, which is beneficial, but it can also decrease the hydrogen flux. A test of HTM films on porous alumina disks [5] showed that flux values were 15-40% lower for Pd/CeO₂ films than for Pd/TZ-3Y films, even though the Pd/TZ-3Y films were \approx 50% thicker. The CeO₂-containing films might have lower flux and permeability values because their higher density impedes hydrogen transport (if gas-phase transport through isolated pores contributes significantly to hydrogen transport), or because the Pd content on their surface is low [5].

Concentration polarization effects are evident in the flux data for both the Pd/ZrO₂ and Pd/CeO₂ tubes. They result from accumulation of hydrogen in a boundary layer near the sweep side of the membrane or from depletion of hydrogen in a layer near the feed surface. In either case, the chemical potential of hydrogen near the surface differs from the chemical potential away from the surface, and the hydrogen flux is no longer a simple function of the hydrogen concentrations in the feed and sweep gases. Concentration polarization effects are expected to be more pronounced when the hydrogen concentration in the feed gas is low, the flow rates of feed and/or sweep gases are low, or the membrane has a high hydrogen permeability. The porous supports for the thin films also favor the development of concentration polarization, because they impede gas transport and facilitate establishment of a boundary layer at the membrane's surface.

Two observations suggest that concentration polarization influenced the flux and permeability measurements for the Pd/TZ-3Y and Pd/CeO₂ tubes. First, flux values for both tubes (Fig. 2) were essentially independent of temperature when 4% H₂/balance He was used as the feed gas. When the feed gas was switched to 90% H₂/balance He, the flux for the Pd/CeO₂ tube increased with temperature, as it should due to the thermally activated nature of permeation. The flux for the Pd/ZrO₂ tube, however, remained independent of temperature even with feed gas of 90% H₂/He, because its higher flux favors concentration polarization. Second, the permeability values for both tubes (Fig. 3) depend strongly on the hydrogen concentration in the feed gas, especially at high temperatures. If concentration polarization were not a factor, the hydrogen concentration in the feed gas would not affect the permeability.

Concentration polarization is also evident in the hydrogen flow rate through the Pd/TZ-3Y tube (Fig. 4), especially for feed gas with 4% H₂ at all flow rates tested and feed gas with 90% H₂ at low sweep-gas flow rate (150 ml/min). Under these conditions, the hydrogen flow rate (Fig. 4) is essentially independent of temperature, and the permeability (Fig. 3) is significantly lower than predicted from literature values for palladium [6]. Figure 3 shows a line for 60% of the permeability value reported for palladium by Koffler et al. [6]. Because the Pd/TZ-3Y tube contains 60 vol.% Pd, this line plots the "expected" permeability values for the tube, if it is assumed that concentration polarization does not affect our measurements. The significant difference between the expected permeability values and Argonne's measured values indicates that concentration polarization is a factor for feed gas with 4% H₂ over a wide flow rate and feed gas with 90% H₂ at low gas flow rate.

Concentration polarization is largely overcome with high hydrogen concentration in the feed gas and high gas flow rates. Whether the feed gas contains 4% or 90% H₂, the flux and permeability values increased significantly when the sweep flow rate increased from 150 to 300 ml/min, and the feed flow rate increased from 150 to 500 ml/min. We are uncertain whether the increase in measured values is related to polarization on the feed side or the sweep side of the membrane, because the feed- and sweep-gas flow rates were increased together. Even with high gas flow rates, however, the permeability values for the feed gas with 4% H₂ are much smaller than the expected values, indicating that concentration polarization remains a factor for feed gas with low hydrogen concentration. By contrast, permeability values were close to the expected values when they were measured with 90% H₂ as the feed gas and sweep-gas flow rate ≥ 300 ml/min, and both flux and permeability increased with temperature, as expected due to the activated nature of hydrogen permeation. These results suggest that concentration polarization is minimized by high gas flow rates and high hydrogen concentration in the feed gas.

Milestone 2. Test tubular membrane in syngas atmospheres.

A tubular ANL-3e membrane was prepared to test its chemical stability in simulated syngas. A porous Al_2O_3 tube for supporting the thin-film membrane was prepared by cold isostatic pressing (procedure described in the previous section). After the tube was pre-sintered for 3-5 h at 800-950°C in air, it was painted with a slurry of ANL-3e components [TZ-3Y with Pd powder (60 vol.%)] and was sintered for 5 h at 1400-1500°C in air. The tube was ≈ 8 cm in length with an outside diameter of ≈ 1.2 cm. The membrane had a thickness of ≈ 30 μm and a surface area of ≈ 29.3 cm^2 .

To measure the hydrogen flux, the tube was mounted on the spring-loaded test fixture described in the previous section. A gold ring was placed between the end of the tubular membrane and the alumina tube used to flow sweep gas. To form a seal between the tubes, the fixture was heated to 950°C and held overnight while flowing high-purity He (99.998%) on the outside of the tube and high-purity N_2 (99.998%) on the inside. The gases were flowed at a rate of 150 ml/min during the sealing procedure. Hydrogen flux measurements were begun after the seal was formed, and the tube was cooled to 725°C.

Feed gas mixtures for the hydrogen flux measurements were prepared by using mass flow controllers (MKS 1179A) to blend appropriate amounts of three gases: ultrahigh purity (UHP) He (99.999%), 518.2 ppm H_2S /balance He, and either a mixture containing 66.1% H_2 , 30.9% CO, and 0.99% CO_2 or high-purity H_2 (99.995%). "Syngas with H_2S " had a composition of 50.0 mol.% H_2 , 23.4% CO, 0.75% CO_2 , 50 ppm H_2S , balance He; it was prepared by mixing 518.2 ppm H_2S /balance He and UHP He with the 66.1% H_2 mixture. "Syngas without H_2S " had the composition 50.0 mol.% H_2 , 23.4% CO, 0.75% CO_2 , balance He.

To assess the magnitude of concentration polarization effects during the measurements, the hydrogen flux was first measured under a range of hydrogen flow rates (≈ 100 -225 cm^3/min) with H_2/He mixtures as the feed gas. During subsequent tests of the tube's chemical stability, the hydrogen concentration in the feed (50 mol.%) and the hydrogen flow rate (132 cm^3/min) were kept constant. High purity nitrogen was used as the sweep gas in all measurements. The flow rate of sweep gas was ≈ 500 cm^3/min (unless otherwise specified). Actual flow rates of individual gases were measured with a Field Cal 570 flow calibrator from Humonics.

The hydrogen and helium concentrations in the sweep gas were measured with an SRI 8610C gas chromatograph. For a given condition, these concentrations were measured four times, and the average of those readings was used to calculate the hydrogen flux. The helium concentration was used to correct flux values for hydrogen leakage through defects in the membrane and/or the seal. The flow rate of the feed gas was ≥ 250 cm^3/min , and the sample chamber had a volume of ≈ 2600 cm^3 ; therefore, a volume of gas equivalent to the volume of the sample chamber flowed into the chamber

in ≈ 10 min, and the gas composition in the sample chamber was expected to equal the feed gas composition within ≈ 1 h of changing gas composition. For each feed gas composition, the first flux measurement was made after at least 1 h to ensure the correct gas composition. Energy dispersive spectroscopy (EDS) for chemical analysis was done with a Voyager system (Thermo Electron Scientific Instruments Corp.) attached to a JEOL 5400 scanning electron microscope (SEM).

Figure 5 shows the hydrogen flux of a tubular ANL-3e membrane versus exposure time in feed gas with various compositions. Data that were collected using feed gas with 50 ppm H_2S are shown by solid symbols; data represented by open symbols were collected using feed gas without H_2S . Considering that the thickness of the membrane is ≈ 30 μm , the flux values are low. We show later that these low flux values result partly from concentration polarization due to low gas flow rates. The hydrogen concentration in the feed gas was 50 mol.%, and the hydrogen flow rate was 132 cm^3/min for all values in Fig. 5. Initial flux values measured with feed gas composed of 50% $\text{H}_2/50\%$ He are not shown because they were measured under different feed-gas flow rates.

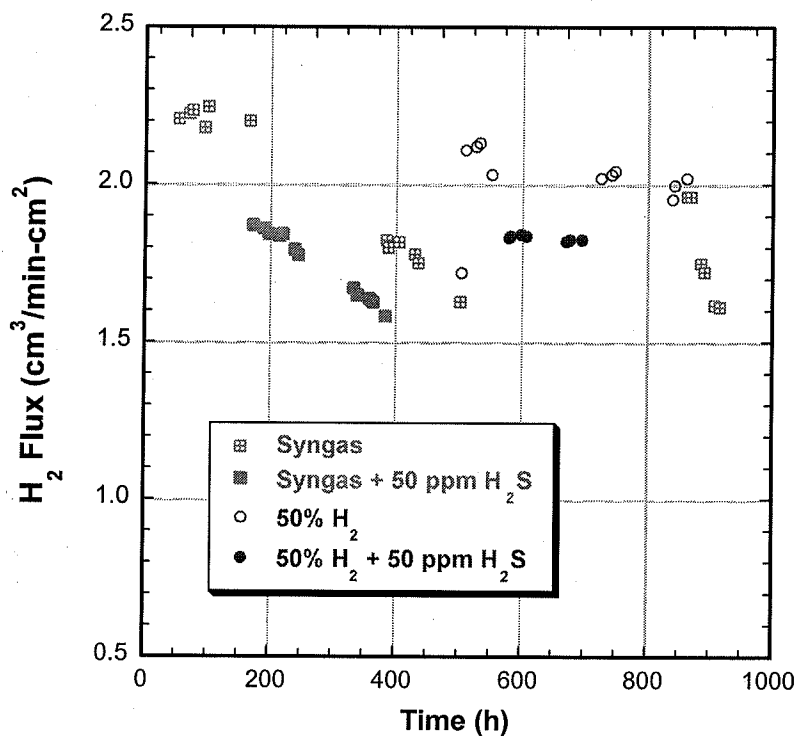


Fig. 5 Hydrogen flux of tubular ANL-3e thin film at 725°C . Measured using feed gas with various compositions and N_2 as sweep gas. The H_2 concentration in the feed (50 mol.%) and the hydrogen flow rate (132 cm^3/min) were constant during the measurements.

The flux was stable for ≈ 115 h during the initial exposure to syngas without H_2S but quickly dropped when 50 ppm H_2S was added to the feed gas (at ≈ 165 h) and steadily decreased during ≈ 220 h of exposure to syngas with H_2S . The hydrogen flux then sharply increased when H_2S was eliminated from the feed gas (at ≈ 385 h), and the magnitude of the increase ($\approx 12\%$) nearly equaled the magnitude of the decrease ($\approx 15\%$) from the introduction of H_2S at ≈ 165 h. Similarly, the hydrogen flux quickly dropped $\approx 10\%$ when 50 ppm H_2S was added to feed gas of 50% H_2 /balance He (at ≈ 560 h), and increased just as quickly by the same amount when H_2S was removed at ≈ 700 h. Disk-shaped ANL-3e membranes also showed a sharp decrease in flux when H_2S was added to the feed gas [7]. Because thermodynamic data [2] indicate that Pd_4S should not form under the conditions of the experiment, we believe that adsorption of H_2S caused the sharp decreases in flux by hindering the membrane's adsorption of hydrogen. Likewise, when H_2S was removed from the feed gas, H_2S desorbed from the membrane, freeing up hydrogen adsorption sites and allowing the flux to quickly increase.

While the sudden flux changes discussed above were probably related to adsorption (or desorption) of H_2S , we believe that a different effect caused the more gradual flux changes that occurred both when H_2S was present (≈ 165 - 385 h) and when it was absent (≈ 385 - 500 h and ≈ 860 - 920 h). A possible cause for the gradual changes is suggested by comparing the response of the flux to three exposures to syngas without H_2S . The flux response during each exposure might be expected to be similar, because the composition of the feed gas was nominally identical; however, each flux response was unique. The flux was essentially constant during the first exposure (≈ 50 - 165 h), decreased steadily during the second exposure (≈ 385 - 500 h), and decreased the most rapidly during the third exposure (≈ 865 - 920 h). The feed gas contained no H_2S before the first exposure to syngas, but it contained 50 ppm H_2S (≈ 165 - 385 h) before the second exposure and again (≈ 560 - 700 h) before the third exposure. After each exposure to feed gas with H_2S , the flux decreased more rapidly during the subsequent exposure to syngas without H_2S . This finding suggests that H_2S played an indirect role in the gradual flux decreases even though it was not the primary cause.

It is reasonable to believe that deposition of coke is related to the gradual decreases in flux that occurred during exposure to syngas without H_2S . After the final exposure to syngas without H_2S , the feed gas was switched to nitrogen, and the furnace was cooled to room temperature at a rate of $180^\circ\text{C}/\text{h}$. When the sample holder was removed from the furnace, coke was seen everywhere within several inches of the membrane (Fig. 6) and in cooler areas where feed gas flowed into and out of the reactor. Also, the flux was nearly constant during the tube's exposure to 50% H_2 /50 ppm H_2S /balance He (≈ 560 - 700 h), when coke deposition was precluded by the absence of carbon-containing gases in the feed gas. Thus, the flux decreased steadily in a feed gas that deposited coke inside the reactor, but was nearly constant in feed gas that could not have deposited coke.

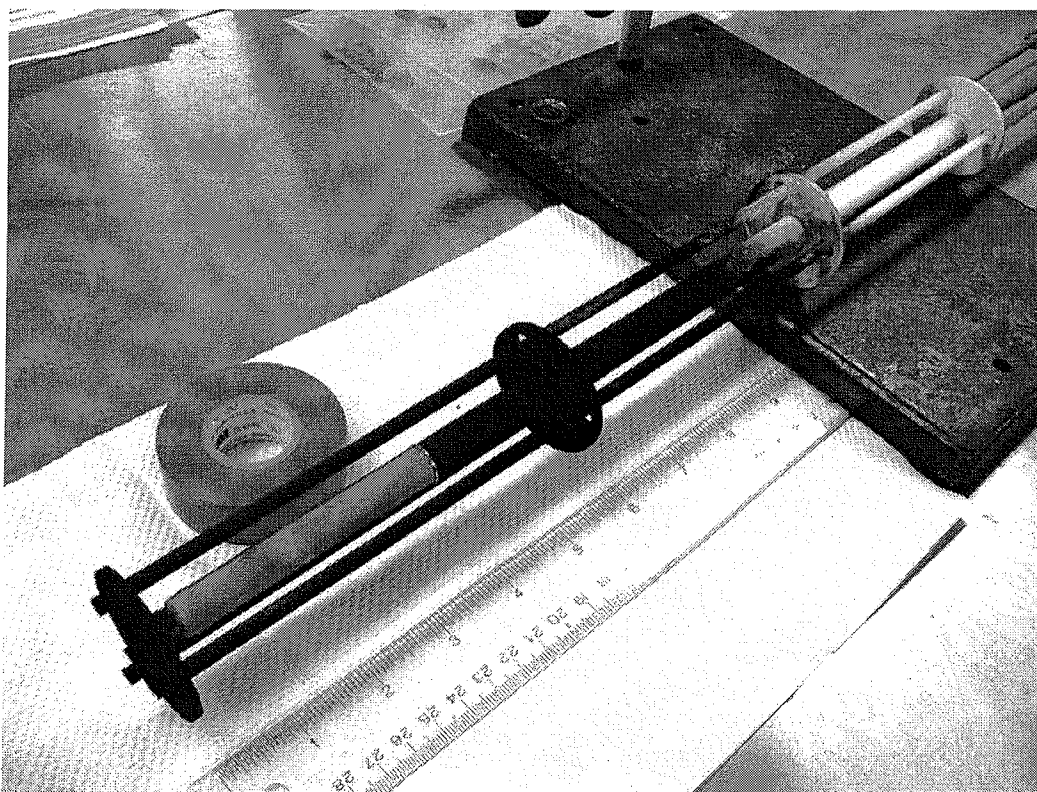


Fig. 6 Sample holder with ANL-3e tube showing coke formation that occurred during measurements of hydrogen flux at 725°C in feed gas with various compositions.

Analysis with EDS showed that the coke (Fig. 6) contained C and Fe ($\approx 5-10$ wt.%). After a coke sample had been collected for chemical analysis, the holder and membrane tube were placed back into the reactor and heated in flowing 8% O₂/balance N₂ for 8 h at 900°C. During the heat treatment, the residue seemed (by visual inspection) to disappear from the sample holder, but it was still abundant at the inlet and outlet of the reactor, and its color converted from black to red (like Fe₂O₃) near the inlet. The presence of Fe in the coke indicates that the feed gas attacked stainless steel components in the gas line during the experiment, and suggests that deposition of coke and Fe is related. In fact, Fe catalyzes coke formation [8]. After the heat treatment in 8% O₂/N₂, Fe was not found (by EDS analysis) on the surface of the membrane tube. This finding is puzzling considering that Fe was found at the inlet and the outlet of the reactor tube. If the decreases in hydrogen flux reflect deposition of coke, as discussed above, the constant flux suggests that coke did not deposit in the reactor during the first exposure to syngas without H₂S ($\approx 50-165$ h). Only after H₂S was added to the syngas (at ≈ 165 h) did the flux begin decreasing gradually. This behavior suggests that H₂S plays an important role in the formation of coke, perhaps by attacking the stainless steel gas lines and facilitating transport of Fe into the reactor, where the Fe catalyzed the deposition of coke.

Table 1 shows the effect of gas flow rates on the hydrogen flux of the ANL-3e tube. For feed gas that contained either 48% H₂/52% He or 50% H₂/50% He, the flux increased considerably as the feed and sweep gas flow rates were increased. This finding agrees with previous results obtained with a different tubular ANL-3e membrane of similar dimensions [2], which also showed an increase in the hydrogen flux as the gas flow rates increased. An increase in flow rates can decrease concentration polarization by preventing the accumulation of hydrogen near the sweep side of the membrane and/or the depletion of hydrogen near the feed side. In the case of the tubes described in a previous report [2] and earlier in this report, concentration polarization is largely overcome with gas flow rates in the range of ≈ 500 cm³/min [2]. During the measurements summarized in Table 1, the maximum hydrogen flow rate for the feed gas was 225 cm³/min; therefore, concentration polarization probably limited the hydrogen flux to some degree. Accordingly, the maximum hydrogen flux for the tube was ≈ 3.4 cm³/min-cm², much lower than was reported [9] for small disks of ANL-3e thin films.

Table 1. Effect of feed and sweep gas flow rates on hydrogen flux of tubular ANL-3e thin-film membrane.

Feed Composition (% H ₂ -% He)	H ₂ Flow Rate in Feed (cm ³ /min)	Sweep Gas (N ₂) Flow Rate (cm ³ /min)	Hydrogen Flux (cm ³ /min-cm ²)
48-52	147	280	2.05
48-52	199	500	2.58
50-50	101	140	1.31
50-50	132	505	2.13
90-10	225	500	3.38

Gas flow rates can also exercise a pronounced effect on hydrogen flux values for disk-shaped thin-film membranes, despite their small active area (≈ 1.3 cm²). Flux is plotted versus inverse temperature (Fig. 7) for a disk-shaped ANL-3e thin film with a thickness of ≈ 18 μ m. In tests using feed gas of 90% H₂/balance He with feed and sweep gas flow rates of 150 cm³/min, the flux at 900°C was approximately 28 cm³/min-cm². This compares favorably with the value of 32 cm³/min-cm² that was measured for another disk-shaped ANL-3e film with similar thickness under the same gas flow rates but with 100% H₂ as the feed gas [1]. When the feed and sweep gas flow rates were increased to 500 cm³/min (Fig. 7), the concentration polarization effects were reduced, and the hydrogen flux at 900°C was increased from ≈ 28 to ≈ 50 cm³/min-cm², the highest value that has been reported to date for an ANL membrane. The higher flow rates increased the hydrogen flux to ≈ 26 cm³/min-cm² at 400°C. Gas flow rates should influence even more profoundly the performance of tubular membranes due to their much larger active areas.

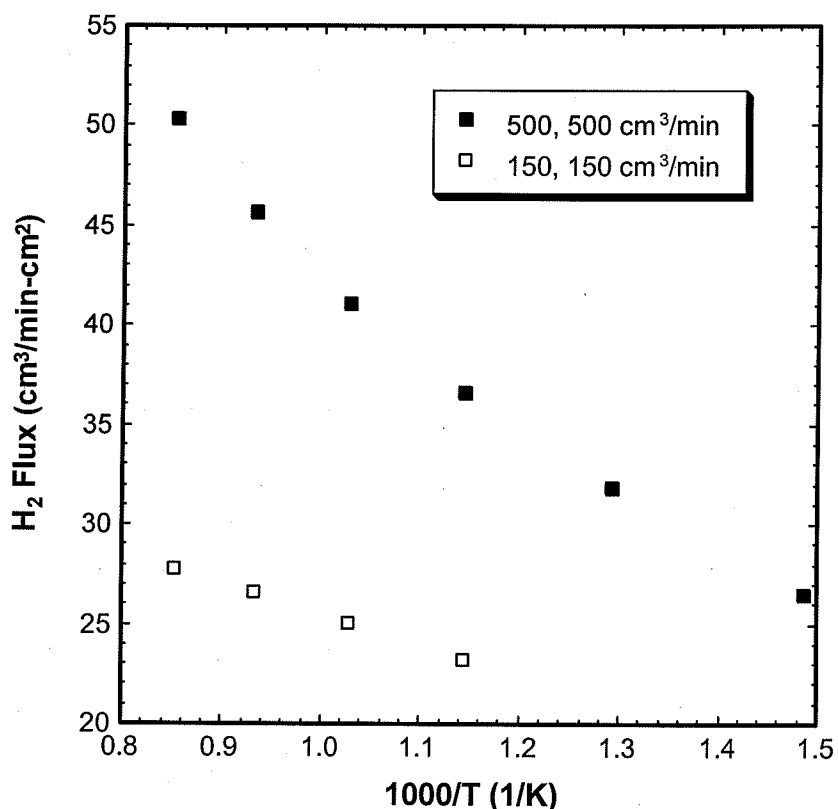


Fig. 7 Hydrogen flux of ANL-3e thin film (thickness $\approx 18 \mu\text{m}$) measured with N_2 as sweep gas and 90% H_2 /balance He as feed gas. Inset gives flow rates for feed and sweep gas during measurements.

Milestone 3. Correlate phase boundary data with hydrogen flux measurements.

Hydrogen flux data for Pd foil samples and self-supporting ANL-3e membranes were correlated with data regarding the Pd/Pd₄S phase boundary. A powder mixture for making ANL-3e membranes was prepared by mixing Pd powder (60 vol.%) with TZ-3Y (i.e., ZrO_2 partially stabilized with Y_2O_3) powder from Tosoh Ceramics. Dense samples were prepared by uniaxially hot-pressing the Pd/TZ-3Y mixture for 25 min at 1150°C in a roughing-pump vacuum. To prepare a disk for flux measurements, 600-grit SiC paper was used to polish the disk's faces flat and parallel to each other. The ANL-3e membranes had a thickness of $\approx 250 \mu\text{m}$ in the first test, $\approx 330 \mu\text{m}$ in the second test, and $\approx 150 \mu\text{m}$ in the third test. The Pd (99.9%) foil samples were made by punching out disks ($\approx 20\text{-mm}$ dia. x 0.1-mm thick) from commercially available foil (Alfa Aesar).

For permeation tests, a sample was mounted on a spring-loaded fixture like the one shown in Figs. 1 and 6. A gold washer was used as a seal between the sample and the alumina tube for passing sweep gas. The sample was heated ($2\text{-}3^\circ\text{C}/\text{min}$) to 920°C while flowing high-purity He on the feed side of the sample and high-purity N_2 on the sweep side to improve the seal. After heating at 920°C , the sample was cooled to 725°C for hydrogen permeation measurements.

Tests at 725°C were done previously [10] with two ANL-3e membranes and two Pd foil samples. New results from tests with a third Pd foil sample and a third ANL-3e membrane are reported here. The feed gas for the tests was prepared by using mass flow controllers (MKS 1179A) to mix three gases: high-purity H₂ (99.995%), ultrahigh purity He (99.999%), and either 513.5 ppm H₂S/balance N₂ or 1006 ppm H₂S/balance He. To calculate the composition of the feed gas, we measured the flow rates of individual gases using a flow calibrator (either Field Cal 570 from Humonics or Agilent 630).

In each test, we fixed the H₂ concentration (10%) in the feed gas while we increased the H₂S concentration incrementally, beginning with an H₂S concentration that was low enough to avoid formation of Pd₄S. After each increment in H₂S concentration, we monitored the flux for at least ≈24 h to judge if the flux was changing. In the recent tests, the flux was monitored for longer time (at least ≈60 h) at each H₂S concentration to better assess whether flux was constant or simply changing slowly.

The flow rate of feed gas was 150 cm³/min during the first two tests with Pd foil and the first two tests with ANL-3e membranes, but was increased to 250 cm³/min during the recent tests. The sample chamber had a volume of ≈2600 cm³; therefore, a volume of gas equivalent to the sample chamber's volume flowed into the chamber in ≈10-17 min, and the composition of gas in the sample chamber was expected to equal the feed gas composition within ≈1 h after changing the feed gas composition. The H₂S concentration was increased in this way in small increments until the flux decreased sharply. This decrease signaled that Pd₄S had formed, and the Pd/Pd₄S phase boundary had been crossed.

At the end of a test, the reactor was held for ≈0.5 h at 725°C while high-purity He was flowed (>100 ml/min) on the feed side and high-purity N₂ was flowed (>100 ml/min) on the sweep side. After holding under these conditions for ≈0.5 h, the flow rates of He and N₂ were reduced to ≈60 ml/min, and the reactor was cooled (3°C/min) to room temperature.

The microstructural features of the membrane were examined with a JEOL 5400 SEM and a Voyager EDS system from Thermo Electron Scientific Instruments Corp. The procedures for measuring hydrogen flux are described elsewhere [11]. For a given condition, the hydrogen and helium concentrations in the sweep stream were measured four times with a gas chromatograph (SRI 8610C), and the average of those readings was used to calculate the hydrogen flux. Individual readings typically varied from the average value by ≤5%. The values of hydrogen flux were corrected for leakage based on the helium concentration measured in the sweep gas.

Figure 8 shows the hydrogen flux for an ANL-3e membrane (thickness ≈250 μm) versus time during which the H₂S concentration in the feed gas was incrementally increased while the hydrogen concentration was held constant (≈10%). The arrows in Fig. 8 indicate when the H₂S concentration was increased to the concentration (ppm) given by the number beneath the arrow. The initial H₂S concentration was ≈50 ppm. At ≈360 h, the flux values decreased suddenly by ≈40%.

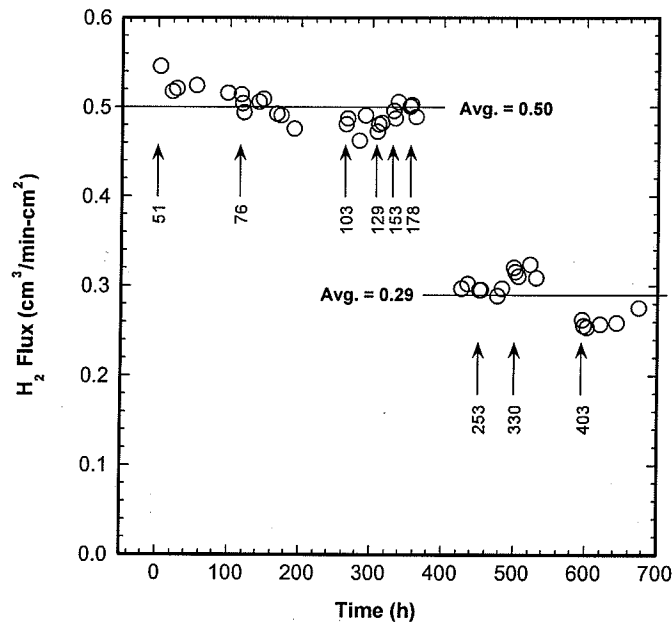


Fig. 8 Hydrogen flux for ANL-3e membrane (thickness $\approx 250 \mu\text{m}$) at $\approx 725^\circ\text{C}$ in feed gas with constant H_2 concentration ($\approx 10\%$) but various H_2S concentrations. Arrows indicate when H_2S concentration was increased to concentration (ppm) given by numbers below arrow.

The flux values (Fig. 8) can be separated into those measured before ≈ 360 h and those measured after ≈ 425 h. The average flux was $0.50 (\pm 5\%) \text{ cm}^3/\text{min-cm}^2$ before ≈ 360 h, and decreased to $0.29 (\pm 10\%) \text{ cm}^3/\text{min-cm}^2$ after ≈ 425 h. The H_2S concentration in the feed gas was ≤ 153 ppm until 353.4 h and then was increased to 178 ppm. The flux was stable for ≈ 24 h in feed gas with 153 ppm H_2S before the H_2S concentration was increased to 178 ppm. With 178 ppm H_2S in the feed, the flux appeared to be stable for ≈ 8 h but fell sharply when it was measured again ≈ 65 h later. No further decrease in flux was seen when the H_2S concentration was increased to 253, 330, and 403 ppm over the final ≈ 250 h of the experiment. Figure 9a shows that a reaction layer with a thickness of $\approx 50 \mu\text{m}$ had formed during the experiment, while Fig. 9b shows that the layer was dense, except for isolated pores dispersed along the grain boundaries. The EDS analysis indicated that the reaction layer's composition was Pd_4S .

The decrease in flux ($\approx 40\%$) during exposure to 178 ppm H_2S is much larger than the experimental uncertainty ($\approx 5\%$) in flux values measured in feed gas with lower H_2S concentrations (i.e., before ≈ 360 h) and the uncertainty ($\approx 10\%$) in values measured in feed with higher H_2S concentrations (i.e., after ≈ 425 h). The large decrease in flux is attributed to the formation of a compact layer of Pd_4S , whose hydrogen permeability is lower than that of Pd. From the results in Fig. 8, the hydrogen permeability of Pd_4S was estimated to be $1.4 \times 10^{-9} \text{ mol/m-s-Pa}^{1/2}$, versus a value of $1.2 \times 10^{-8} \text{ mol/m-s-Pa}^{1/2}$ for the membrane's permeability before Pd_4S formed.

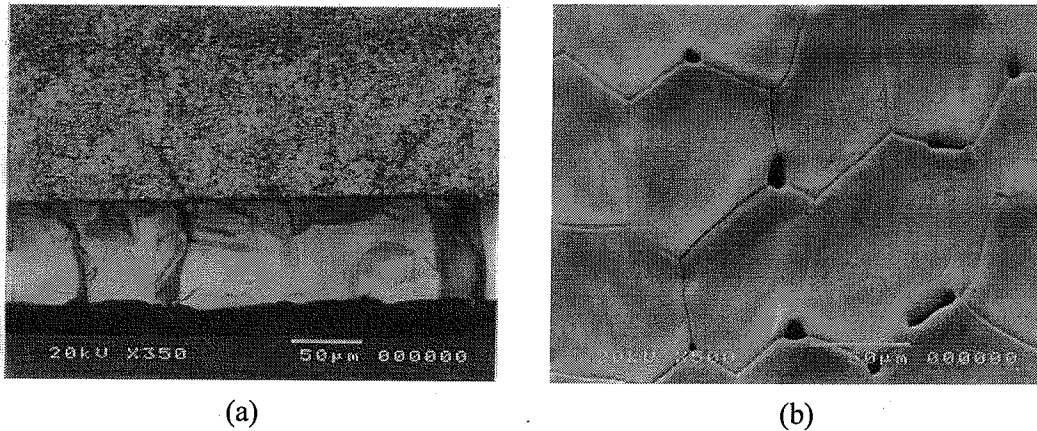


Fig. 9 Secondary electron images of ANL-3e membrane used to collect data in Fig. 8: (a) cross-sectional view of $\approx 50\text{-}\mu\text{m}$ -thick layer of Pd_4S (below) on membrane's surface (above), and (b) top view of Pd_4S layer showing isolated porosity at its grain boundaries.

After the compact layer of Pd_4S formed, causing the sharp decrease in hydrogen flux, further formation of Pd_4S was limited by the diffusion of Pd from the membrane's interior, as suggested by two observations. First, the flux did not decrease during the final 250 h of the experiment, meaning that the thickness of the Pd_4S layer did not increase significantly. This finding is consistent with diffusion-limited, parabolic reaction kinetics. Second, the reaction layer (Fig. 9a) contained only Pd_4S . If diffusion of sulfur into the membrane's interior had limited the formation of Pd_4S , rather than the diffusion of Pd to the surface, the reaction layer would have contained a mixture of Pd_4S and ZrO_2 .

For ANL-3e membranes in feed gas with 10% H_2 , the flux values in Fig. 8 suggest that Pd is stable at 725°C in feed containing 153 ppm H_2S , whereas Pd_4S is stable for feed containing 178 ppm H_2S . This finding indicates that the Pd/ Pd_4S phase boundary lies between 153 and 178 ppm H_2S . To test these results, a second experiment was done with a slightly thicker ANL-3e membrane (thickness of $\approx 330\ \mu\text{m}$). The hydrogen flux was initially measured using feed with no H_2S and then with 155 ppm H_2S (while the hydrogen concentration was held constant at 10%). As soon as the H_2S concentration in the feed gas was increased from 0 to 155 ppm, the flux decreased sharply (Fig. 10), indicating that the phase boundary lies at ≤ 155 ppm H_2S . Figure 11 plots this result with the Pd/ Pd_4S phase boundary data determined previously [2] by examining ANL-3e samples after their exposure to feed gas with a fixed H_2 concentration and various H_2S concentrations. The present result agrees well with the earlier results.

The hydrogen flux was also measured versus time for two samples of Pd foil (thickness $\approx 100\ \mu\text{m}$) while the H_2S concentration in the feed gas was incrementally increased with the hydrogen concentration fixed at $\approx 10\%$. Figure 12 shows the results for a foil sample exposed to 0, 51, 103, and 155 ppm $\text{H}_2\text{S}/10\%$ $\text{H}_2/\text{balance He+N}_2$. The arrows in the figure show when the H_2S concentration was increased to the concentration (ppm) given beneath the arrow.

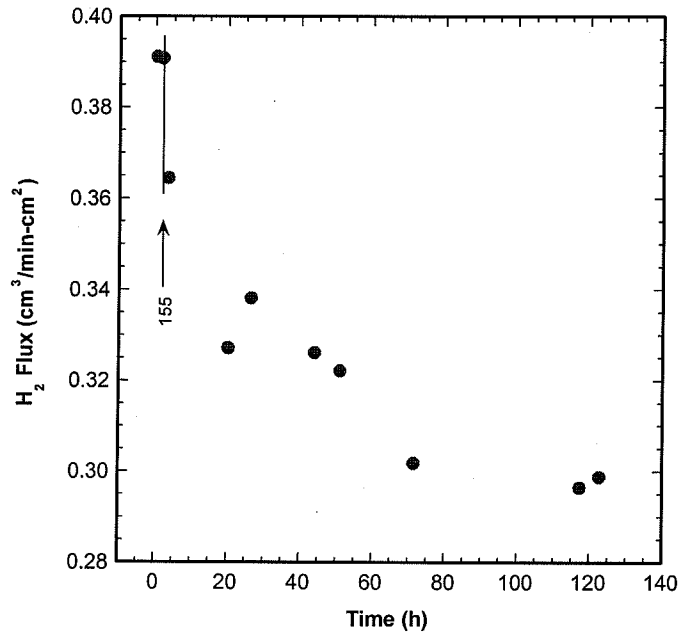


Fig. 10 Hydrogen flux for 330- μm -thick ANL-3e membrane at 725°C in feed gas whose H_2S concentration was increased from 0 to 155 ppm at time indicated by arrow. Hydrogen concentration kept constant at $\approx 10\%$.

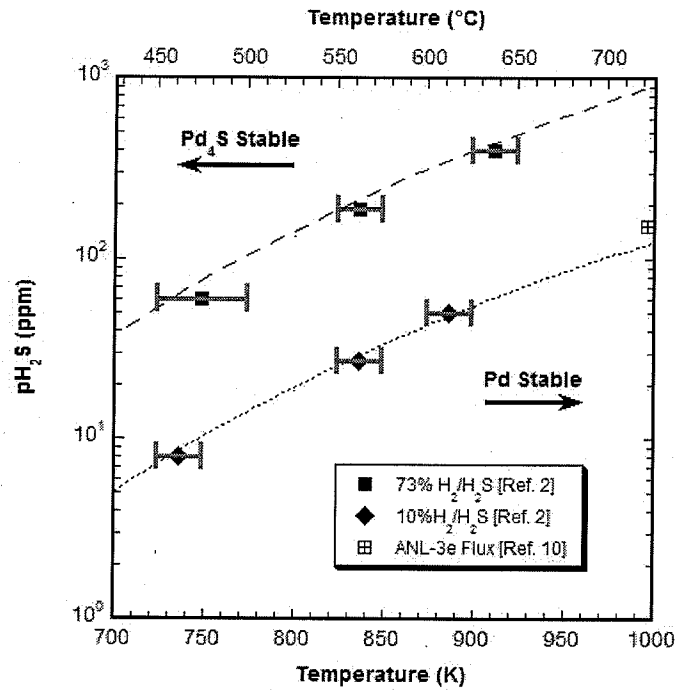


Fig. 11 Determination of Pd/Pd₄S phase boundary for tests at different temperatures and H_2S concentrations. Solid points were determined [2] by equilibrating samples under various conditions. Dashed lines are fits of those data. Open point was determined by measuring flux while increasing H_2S concentration.

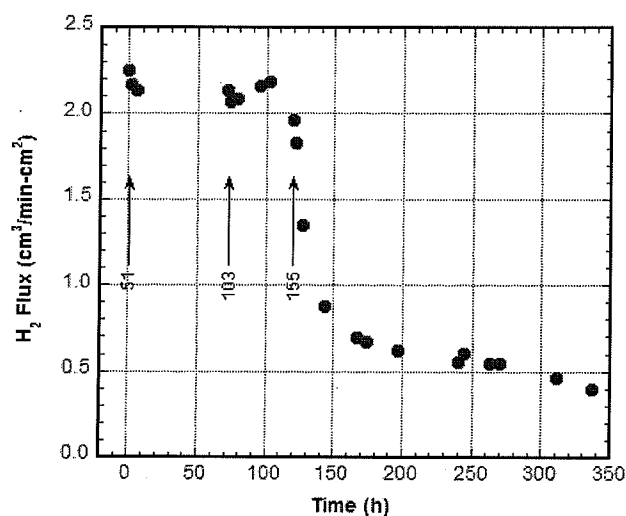


Fig. 12 Hydrogen flux for Pd foil at $\approx 725^\circ\text{C}$ in feed gas with constant H_2 concentration ($\approx 10\%$) but various H_2S concentrations, initially 0 ppm. Arrows indicate when H_2S concentration was increased to concentration (ppm) given by number next to arrow.

Figure 12 shows a flux of $2.25 \text{ cm}^3/\text{min-cm}^2$ with 10% H_2 /balance He (no H_2S) as feed gas. When the H_2S concentration in the feed gas was increased to 51 ppm, the flux decreased to $2.17 \text{ cm}^3/\text{min-cm}^2$ but remained steady for ≈ 72 h, at which point the H_2S concentration was increased to 103 ppm. With an H_2S concentration of 103 ppm, the flux initially dropped to $2.06\text{-}2.08 \text{ cm}^3/\text{min-cm}^2$ before it increased to $2.19 \text{ cm}^3/\text{min-cm}^2$. Up to this point in the experiment, the flux values appeared to exhibit a typical variation of $\pm 5\%$ due to experimental uncertainty. In feed gas with 103 ppm H_2S , the final flux value ($1.96 \text{ cm}^3/\text{min-cm}^2$) differed from the average value ($2.15 \text{ cm}^3/\text{min-cm}^2$) by somewhat more than typical. This difference might indicate that Pd_4S had begun to form during exposure to feed gas with 103 ppm H_2S .

Although we are not certain whether the flux of $1.96 \text{ cm}^3/\text{min-cm}^2$ resulted from anomalously large experimental uncertainty or from the incipient formation of Pd_4S , the decrease in flux was sharp and dramatic when the H_2S concentration in the feed gas was increased to 155 ppm. The flux decreased $\approx 65\%$ within ≈ 48 h of introducing feed gas with 155 ppm H_2S , and it continued to decrease an additional 40% over the final 170 h of the experiment. The flux never reached a steady value in the manner that ANL-3e membranes did.

A second Pd foil gave a steady flux of $\approx 2.3 \text{ cm}^3/\text{min-cm}^2$ for ≈ 24 h (Fig. 13) in feed gas containing 78 ppm H_2S , but its flux dropped precipitously after introducing feed gas with 102 ppm H_2S . The results from the first experiment for Pd foil (Fig. 12) suggest that the Pd/ Pd_4S phase boundary is located between ≈ 100 and 155 ppm H_2S for feed gas containing 10% H_2 , whereas the second experiment suggests that the boundary lies between 78 and 102 ppm H_2S . Taken together, the experiments indicate that the Pd/ Pd_4S boundary is probably located near 100 ppm H_2S .

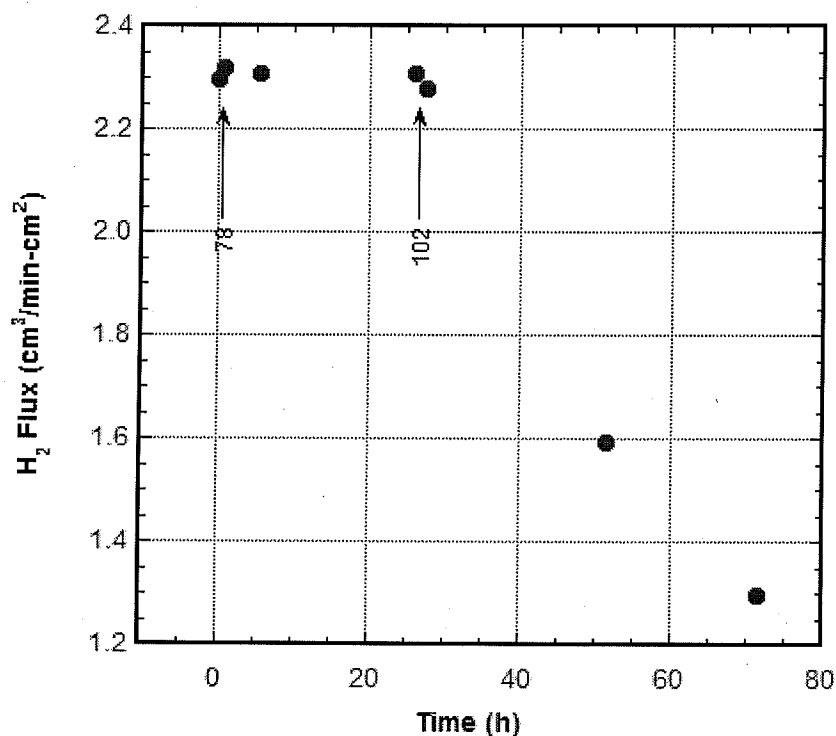


Fig. 13 Hydrogen flux for second Pd foil at $\approx 725^\circ\text{C}$ in feed gas with constant H_2 concentration ($\approx 10\%$) but various H_2S concentrations, initially 0 ppm. Arrows indicate when H_2S concentration was increased to concentration (ppm) given by number next to arrow.

The results discussed to this point, which were reported previously [10], seem to indicate that ANL-3e membranes behave differently than Pd foil during exposure to H_2S . To confirm whether the apparent differences are reproducible, another Pd foil sample and another ANL-3e sample were tested.

In the experiment with Pd foil, the H_2S concentration was increased in stepwise fashion from 0 to 70, 85, and then 100 ppm H_2S in feed gas of 10% H_2 /balance He. During the exposure to 70 ppm H_2S , both the hydrogen flux (Fig. 14) and helium leakage (Fig. 15) were stable for 96 h. After increasing the H_2S concentration to 85 ppm, the helium leakage began increasing. After ≈ 180 h, leakage accounted for $\approx 30\%$ of the hydrogen concentration in the sweep gas; however, after correcting for leakage, we found that the hydrogen flux had decreased only slightly. Likewise, when the H_2S concentration in the feed was increased to 100 ppm, the leakage continued to increase sharply while the hydrogen flux decreased only slightly. After ≈ 29 h with 100 ppm H_2S in the feed, the hydrogen concentration due to leakage was $\approx 40\%$ of the hydrogen in the sweep gas. It is very difficult to correct the hydrogen flux for leakage when the leakage rate is so high; therefore, the experiment was stopped, even though the hydrogen flux had not decreased as sharply as in previous experiments (Figs. 12 and 13).

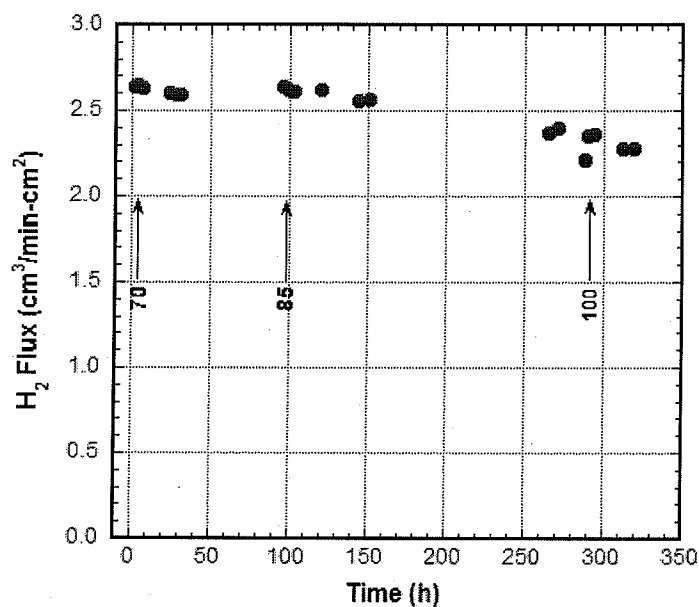


Fig. 14 Hydrogen flux through third Pd foil at 725°C in feed gas with 10% H₂ and various H₂S concentrations. Arrows indicate when H₂S concentration was increased to concentration (ppm) given by number beneath arrow.

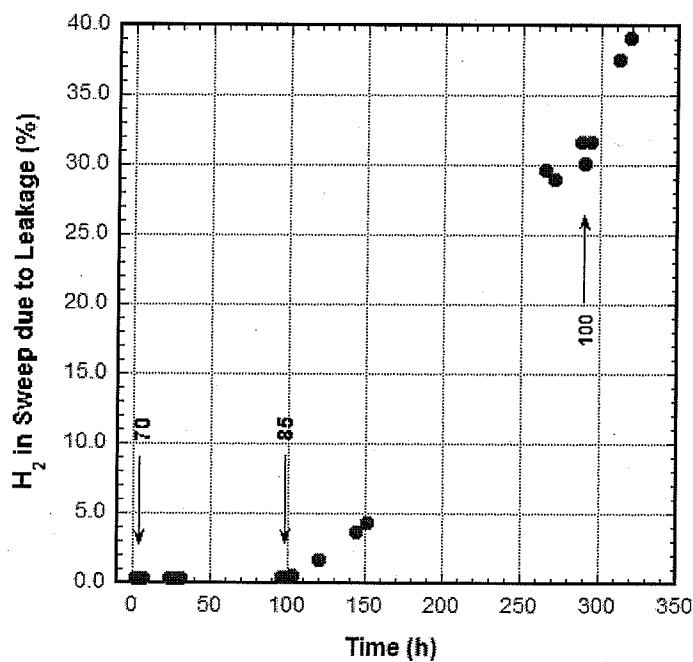


Fig. 15 Percentage of H₂ in sweep gas attributed to leakage during flux measurements with third Pd foil at 725°C in feed gas with 10% H₂ and various H₂S concentrations. Arrows mark times when H₂S concentration was increased to concentration (ppm) given by number near arrows.

Post-test examination of the Pd foil showed an obvious change in its surface morphology, from a smooth surface before the test (Fig. 16a) to a rough surface with many pinholes distributed over its entire surface afterwards (Fig. 16b). Larger pinholes were also seen at the edge of the foil's exposed surface (Fig. 16c) near the alumina plate that held the foil in place on the test fixture. Slightly pressurizing (2-3 psig He) the test fixture after the test and then submerging the sample and gold seal in alcohol showed that helium leaked mostly, if not entirely, through the foil and not through the seal. An EDS analysis after the test showed only Pd on the sample's surface; sulfur was not detected.

The absence of a sharp decrease in flux (Fig. 14) suggests that Pd₄S did not form on the third Pd foil during its exposure to feed gas with 100 ppm H₂S. This inference was borne out by SEM/EDS results that gave no evidence of Pd₄S on the foil's surface after the test. Like the results from the first experiment with Pd foil (Fig. 12), these data indicate that the Pd/Pd₄S phase boundary lies at >100 ppm H₂S for feed gas with 10% H₂. The large increase in leakage during exposure to feed gas with ≥85 ppm H₂S, however, combined with the development of numerous pinholes and significant surface roughening during the test, suggests that 85 ppm H₂S seriously damaged the foil even though Pd₄S did not form. This supports our earlier conclusion [10] that the exposure limit for Pd foil is ≈100 ppm H₂S at 725°C in feed gas with 10% H₂.

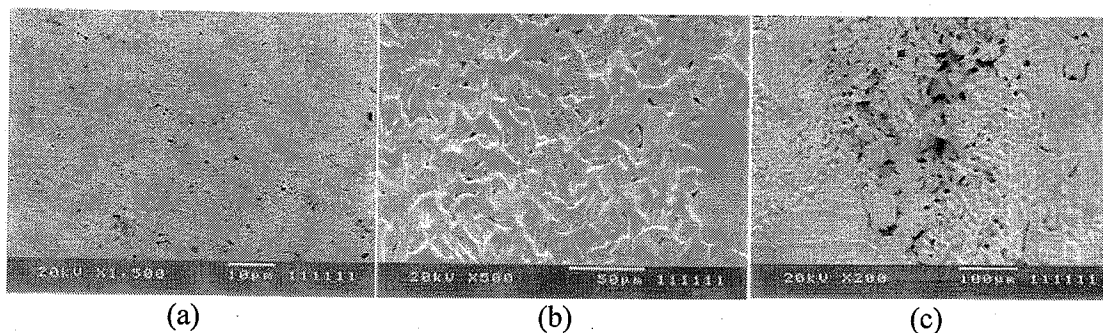


Fig. 16 Secondary electron images of Pd foil before (a) and after (b and c) its flux was measured at 725°C in feed gas with 10% H₂ and various H₂S concentrations.

As with the two previous ANL-3e samples [10], the third sample demonstrated better resistance to H₂S poisoning compared to Pd foil samples. Its flux (Fig. 17) decreased ≈15% when 100 ppm H₂S was first introduced in the feed stream but then remained stable over a period of ≈350 h while the H₂S concentration was increased incrementally to 175 ppm. The flux was stable for ≈96 h in feed with 175 ppm H₂S. The first significant decrease in flux occurred after the H₂S concentration was increased to 200 ppm. After the sample was exposed to 200 ppm H₂S overnight, the reactor was flushed and cooled in flowing inert gas. Examination of the sample with SEM showed numerous particles distributed uniformly over its surface (Fig. 18). An EDS analysis showed that the particles contained Pd (>50 mol.%) with various amounts of sulfur, zirconium, and oxygen.

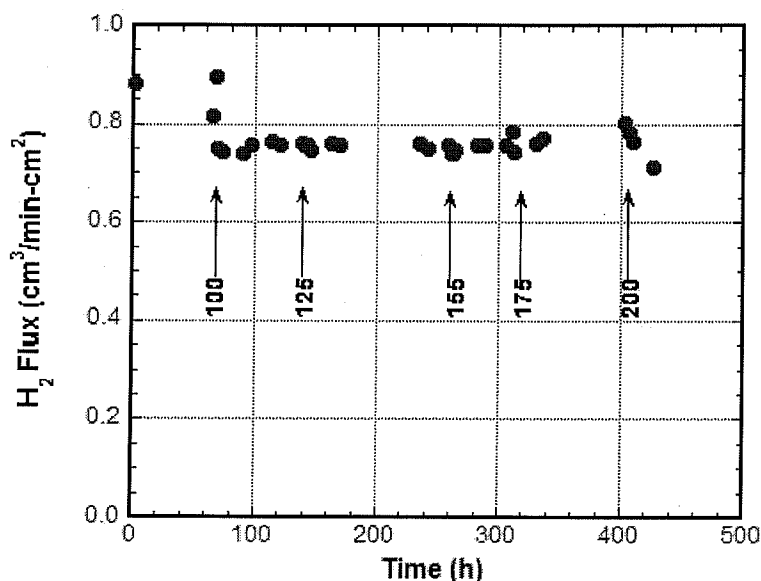


Fig. 17 Hydrogen flux of ANL-3e membrane (thickness $\approx 150 \mu\text{m}$) at 725°C in feed gas with 10% H_2 and various H_2S concentrations. Arrows mark times when H_2S concentration was increased to concentration (ppm) given by number near arrows.

The presence of Pd-rich particles with various concentrations of sulfur suggests that the incipient formation of Pd_4S was interrupted by termination of the experiment after a relatively brief, overnight exposure to 200 ppm H_2S . In agreement with earlier results (Fig. 8), these results indicate that the Pd/ Pd_4S phase boundary for ANL-3e membranes lies in the range 175-200 ppm H_2S at 725°C with feed of 10% H_2 /balance He. Also in agreement with earlier results, the phase boundary for the ANL-3e membrane appears shifted toward higher H_2S concentration relative to the phase boundary for Pd foil. Compared to Pd foil, the ANL-3e sample also showed a much smaller increase in leakage during the exposure to H_2S , increasing to a maximum of $\approx 3\%$ and then beginning to decrease at the end of the test. For this sample, it was not determined whether the leakage was through the sample, the seal, or both.

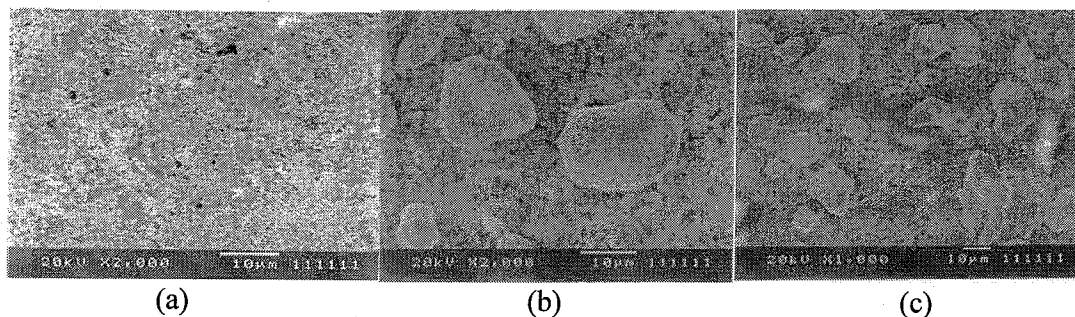


Fig. 18 Secondary electron images of ANL-3e membrane (thickness $\approx 150 \mu\text{m}$) before (a) and after (b and c) its flux was measured at 725°C in feed gas with 10% H_2 and various H_2S concentrations.

The Pd foil and ANL-3e samples exhibit several important similarities and differences in their responses to feed gas with H₂S. For both Pd foil and ANL-3e samples, H₂S affects the flux minimally if its concentration is less than that necessary to form Pd₄S, i.e., if the H₂S concentration lies on the Pd side of the Pd/Pd₄S phase boundary. When Pd₄S forms, the effect on flux is significant for both types of sample; however, Pd foil and ANL-3e samples reacted differently to the formation of Pd₄S. Whereas ANL-3e samples seemed to reach a stable lower flux value after Pd₄S formed, the flux through Pd foil samples continued to decrease. Experiments will be done to follow the evolution of the flux to determine if this apparent difference persists at longer time.

Another apparent difference between ANL-3e and Pd foil samples involves the Pd/Pd₄S phase boundary. The phase boundary was located at ≈150 ppm H₂S for ANL-3e membranes but ≈100 ppm H₂S for Pd foil, i.e., ANL-3e membranes appeared more resistant to formation of Pd₄S. It is not known how the Pd chemical stability might be enhanced in ANL-3e membranes, but the support for Pd-based catalysts can enhance the catalyst's resistance to deactivation from H₂S and other sulfur-containing contaminants [12, 13]. The difference might also be related to the kinetics for Pd₄S formation. The phase boundary is determined by the decrease in hydrogen flux that accompanies the formation of Pd₄S, which requires the diffusion of Pd from the membrane's interior. The diffusion of Pd to the surface is impeded in ANL-3e membranes, because ZrO₂ makes for a more tortuous diffusion path. To properly determine the location of the phase boundary, sufficient time must be allowed for Pd diffusion and formation of Pd₄S.

Additional Effort: Effect of Sintering Aids on Microstructure of Thin-Film HTM

Porosity can profoundly influence the properties of an HTM. Interconnected porosity increases leakage through a membrane, because it allows passage of multiple gas species, depending on the physical dimensions of the porosity and the gas molecule. Porosity that is not interconnected, on the other hand, can enhance hydrogen transport without increasing leakage, because only hydrogen accesses this porosity isolated at the membrane's interior, and transport through the gas phase is much faster than transport through the solid state. A plausible explanation for the better performance of Pd/TZ-3Y membranes, relative to those composed of Pd/CeO₂, is that Pd/TZ-3Y membranes contain more non-interconnected porosity [9].

To test the effect of porosity on the performance of our HTMs, several materials (MgF₂, LiF, BaF₂, CeO₂, and ZnO) were screened as possible sintering aids that could enhance densification and reduce porosity in Pd/TZ-3Y films. Each additive (5-10 wt.%) was mixed with Pd (60 vol.%) / TZ-3Y powder. The powder mixtures with additives were used to make films on porous alumina disks by using our paste-painting technique, and then the film was sintered under standard conditions (5 h in air at 1400 or 1430°C). After testing the sintered films for penetration by isopropyl alcohol (IPA), we examined their microstructures for differences in porosity contents. Micrographs from films with CeO₂ and MgF₂ are compared to a "base" film in Fig. 19.

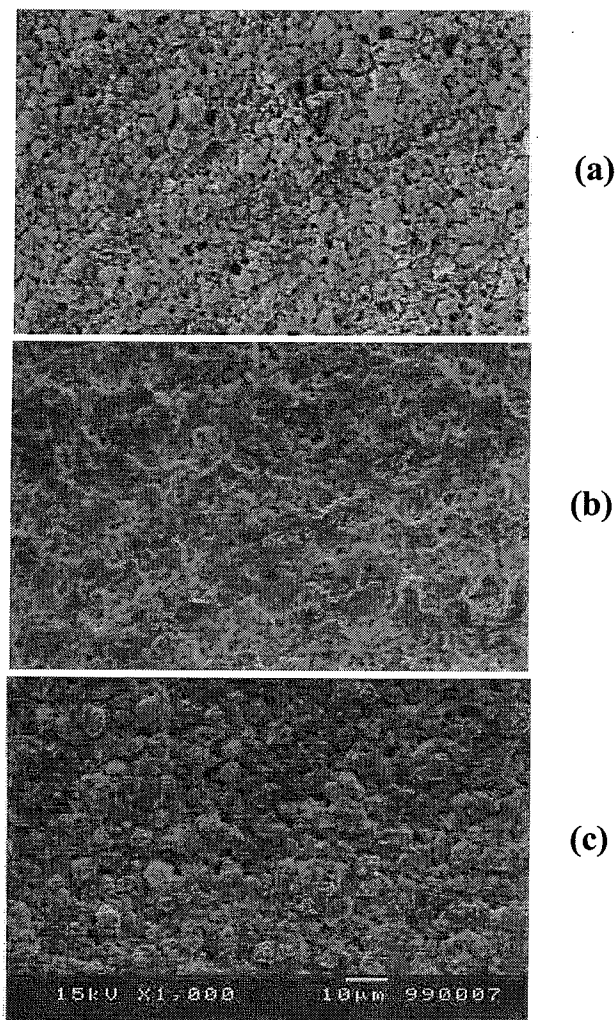


Fig. 19 Plan views of Pd/TZ-3Y films on porous alumina with (a) no additive ("base" film), (b) 10 wt.% MgF₂, and (c) 10 wt.% CeO₂. All were sintered for 5 h at 1400°C in air.

Table 2 summarizes the efficacy of the various additives as sintering aids based on IPA-penetration tests and microstructural evaluations. In terms of their porosity, films made with 10 wt.% LiF, 10 wt.% BaF₂, or 5 wt.% ZnO appeared similar to "base" Pd/TZ-3Y films made without any additive; therefore, these films were excluded from further consideration. The differences in microstructure are not dramatic, but films with 10 wt.% CeO₂ or MgF₂ appear to have less porosity, as do films made with 10 wt.% ZnO. The results have not been entirely consistent, however, requiring further testing of the additives. When the additives consistently reduce porosity in Pd/TZ-3Y films, relative to films made without an additive, the hydrogen flux will be measured to determine if the film performance has been degraded by the reduction in porosity.

Table 2. Effect of various additives on porosity of Pd (60 vol. %)/TZ-3Y thin films on porous Al₂O₃ disks sintered at 1400°C for 5 h in air, compared to “base” film, i.e., film made with no additive.

Additive	Conclusion from Tests
ZnO (5 wt.%)	Appeared similar to “base” film
ZnO (10 wt.%)	Appeared denser than “base” film
CeO ₂ (10 wt.%)	Appeared denser than “base” film
LiF (10 wt.%)	Appeared similar to “base” film
BaF ₂ (10 wt.%)	Appeared similar to “base” film
MgF ₂ (10 wt.%)	Appeared denser than “base” film

V. FUTURE WORK

Development of Tubular HTMs. We will work to increase the effective area of tubular HTMs to assess whether they can be made into practical devices. Although HTM tubes can be fabricated as either self-supporting tubes composed entirely of HTM components or as thin films on porous tubular supports, we will focus on fabricating HTM thin films on porous supports, because they have produced the most promising results. Paste painting has been an effective method for depositing HTM thin films, but other methods (e.g., dip coating or spray deposition) might also be tested for fabricating thinner, stronger, more defect-free thin films. We will continue testing the performance of tubular HTMs in gases that simulate the atmosphere in “real-life” gasifiers. This might include testing HTM tubes in Argonne’s high pressure reactor according to the test protocol developed at the 2008 contractor’s review meeting at NETL. The hydrogen flux and permeability of tubular membranes will be measured as a function of sweep and feed gas flow rates to determine whether concentration polarization is a factor.

Membrane Stability. We will test the ability of Argonne’s HTMs to withstand conditions that are anticipated during coal gasification and/or methane reforming. We will continue testing the HTM’s chemical stability in simulated gasifier atmospheres and will initiate testing of its “cyclability”, i.e., its ability to withstand cyclical changes in temperature and/or hydrogen concentration in the feed gas. We will continue correlating hydrogen flux measurements with Pd/Pd₄S phase boundary data in order to better understand the effect of H₂S-containing atmospheres on the performance of HTMs. Correlations will be made between flux and phase boundary data collected at low temperatures (<700°C). In particular, we will compare the hydrogen flux when Pd₄S is stable to that when Pd is stable. To compare the behavior of Argonne’s cermet membranes to metallic membranes, we will measure the hydrogen flux for both cermet and metallic membranes on both sides of the phase boundary.

High-Pressure Testing. We will use Argonne's high-pressure reactor to test Argonne's membranes according to the protocol that was presented at the H₂-from-coal separations project review meeting at NETL. Because previous high-pressure measurements indicate that the flow rates of feed and sweep gases influence the flux under some conditions, we will investigate the effects of sweep and feed gas flow rates during our high-pressure flux measurements. The fixture for making high-pressure measurements has been modified to enable the testing of disk-shaped thin-film HTMs on porous supports and should allow the testing of HTM tubes.

System Analyses. The Aspen Plus[®] Simulation module will be used to evaluate the economics of an integrated gasification and combined cycle (IGCC) system for hydrogen production that employs HTMs for hydrogen purification. In our evaluation, we will compare the economics of an IGCC system operating at 900°C to one operating at 400°C. In addition to identifying novel equipment, estimating its cost, and considering challenges with interfacing the equipment with the overall system, we will explore opportunities to improve the overall process. In particular, heat source temperature, pressure and duty requirements, heat carrier medium, and conditions and purity of the process streams will be considered. While most of the plant will be based on well-understood equipment, we will need to develop user modules for the HTM units, because they represent a departure from commonly used equipment.

Evaluation of process issues and economics will continue as technical progress warrants. As directed through consultations with NETL's program managers, contacts will be made and discussions will be held with potential collaborators. We will work with NETL's in-house R&D team and their Systems Engineering Group to validate the process concept and conduct techno-economic evaluation of proton-conducting membrane technology for separating hydrogen in the power and petrochemical industries. We will provide technical input and engineering data to the NETL team to develop models for process viability and for thermal management studies.

VI. PUBLICATIONS AND PRESENTATIONS

Transport Properties of $\text{BaCe}_{0.95}\text{Y}_{0.05}\text{O}_{3-\alpha}$ Mixed Conductors for Hydrogen Separation, *Solid State Ionics*, 100, 45 (1997).

Development of Mixed-Conducting Oxides for Gas Separation, *Solid State Ionics*, 108, 363 (1998).

Development of Proton-Conducting Membranes, presented at the AIChE Annual Meeting, New Orleans, LA, March 9-13, 1998.

Mixed-Conducting Ceramic Membranes for Hydrogen Separation, presented at the 193rd Meeting of the Electrochemical Society, San Diego, CA, May 3-8, 1998.

Development of Mixed-Conducting Ceramic Membranes for Hydrogen Separation, *Ceramic Transactions*, 92, 1 (1998).

Development of Mixed-Conducting Dense Ceramic Membranes for Hydrogen Separation, Proc. 5th Intl. Conf. Inorganic Membranes, Nagoya, Japan, June 22-26, 1998, pp. 192-195.

Development of Proton-Conducting Membranes for Hydrogen Separation, presented at the Advanced Coal-based Power and Environmental Systems '98 Conference, Morgantown, WV, July 21-23, 1998.

The Effects of Dopants and A:B Site Nonstoichiometry on Properties of Perovskite-Type Proton Conductors, *J. Electrochem. Soc.*, 145, 1780 (1998).

Transport Properties of $\text{SrCe}_{0.95}\text{Y}_{0.05}\text{O}_{3-\alpha}$ and its Application for Hydrogen Separation, *Solid State Ionics*, 110, 303 (1998).

High-Temperature Deformation of $\text{BaCe}_{1-x}\text{Y}_x\text{O}_{3-y}$ ($0.05 < x < 0.2$), *Solid State Ionics*, 117, 323 (1999).

Development of Mixed-Conducting Ceramics for Gas Separation Applications, *Mat. Res. Soc. Symp. Proc.*, 548, 545 (1999).

Performance Testing of Hydrogen Transport Membranes at Elevated Temperatures and Pressures, presented at Symposium on Hydrogen Production, Storage, and Utilization, New Orleans, Aug. 22-26, 1999; *Am. Chem. Soc., Fuel Chem. Div.*, 44(4), 914 (1999).

Development of Mixed-Conducting Ceramic Membrane for Hydrogen Separation, presented at Sixteenth Annual International Pittsburgh Coal Conference, Pittsburgh, PA, Oct. 11-15, 1999.

Characterization of Ceramic Hydrogen Separation Membranes Containing Various Nickel Concentrations, presented at the Conference on Fossil Energy Materials -- Critical Supporting Technology R&D for Vision 21, Knoxville, TN, April 24-25, 2000.

Mixed Proton-Electron Conducting Cermet Membranes for Hydrogen Separation, presented at 102nd Annual Mtg. of the American Ceramic Society, St. Louis, MO, April 30-May 3, 2000.

Effect of Surface Modification on Hydrogen Permeation of Ni-BaCeO₃ Composites, presented at 102nd Annual Mtg. of the American Ceramic Society, St. Louis, MO, April 30-May 3, 2000.

Effect of Surface Modification on Hydrogen Permeation of Ni-BaY_xCe_{1-x}O_{3-δ} Composites, presented at 197th Meeting of the Electrochemical Society, Toronto, Ontario, Canada, May 14-19, 2000.

Evaluation and Modeling of a High-Temperature, High Pressure, Hydrogen Separation Membrane for Enhanced Hydrogen Production from the Water-Gas Shift Reaction, in "Advances in Hydrogen Energy," eds., C. E. G. Padro and F. Lau, Kluwer Academic/Plenum, New York, pp. 93-110 (2000).

Characterization of Ceramic Hydrogen Separation Membranes with Varying Nickel Concentrations, *J. of Applied Surface Science*, 167, 34 (2000).

The Crystal Structures and Phase Transitions in Y-doped BaCeO₃: Their Dependence on Y-Concentration and Hydrogen Doping, *Solid State Ionics*, 138, 63 (2000).

Development of Dense Ceramic Membranes for Hydrogen Separation, Proc. 26th International Conference on Coal Utilization and Fuel Systems, Clearwater, FL, March 5-8, 2001, pp. 751-761.

Thin-Film Cermet Membrane Preparation for Hydrogen Separation, presented at 103rd Annual Meeting of the American Ceramic Society, Indianapolis, IN, April 22-25, 2001.

Surface Modifications of Hydrogen-Separation Membranes Based on the Mixed Conductor Ni-BCY, presented at 103rd Annual Meeting of the American Ceramic Society, Indianapolis, IN, April 22-25, 2001.

Development of Dense Ceramic Membranes for Hydrogen Separation, published in the Proceedings of the 6th Natural Gas Conversion Symposium, Girdwood, Alaska, June 17-22, 2001.

Development of Dense Ceramic Membranes for Hydrogen Separation, Proceedings of the 18th International Pittsburgh Coal Conference, Newcastle, Australia, Dec. 4-7, 2001, published by the Pittsburgh Coal Conference, University of Pittsburgh, Pittsburgh, PA.

Defect Chemistry Modeling of High-Temperature Proton-Conducting Cerates, *Solid State Ionics*, 149, 1 (2002).

Current Status of Dense Ceramic Membranes for Hydrogen Separation, Proceedings of the 27th International Technical Conference on Coal Utilization and Fuel Systems, Clearwater, FL, March 4-7, 2002, published by the Coal Technology Association, Gaithersburg, MD.

Dense Ceramic Membranes for Hydrogen Separation, presented at the 16th Annual Conference on Fossil Energy Materials, Baltimore, MD, April 22-24, 2002.

Hydrogen Production by High-Temperature Water Splitting Using Mixed Oxygen Ion-Electron Conducting Membranes, Proc. 201st Electrochem. Soc. Mtg., Philadelphia, PA, May 12-17, 2002.

Effect of Pd Coating on Hydrogen Permeation of Ni-Barium Cerate Mixed Conductor, *Electrochemical and Solid-State Letters*, 5(3), J5 (2002).

Electrical Properties of p-type Electronic Defects in the Protonic Conductor $\text{SrCe}_{0.95}\text{Eu}_{0.05}\text{O}_{3-\delta}$, *J. Electrochem. Soc.*, 150(6), A790 (2003).

Interfacial Resistances of Ni-BCY Mixed-Conducting Membranes for Hydrogen Separation, *Solid State Ionics*, 159, 121 (2003).

Defect Structure and n-Type Electrical Properties of $\text{SrCe}_{0.95}\text{Eu}_{0.05}\text{O}_{3-\delta}$, *J. Electrochem. Soc.*, 150, A1484 (2003).

Hydrogen Production by Water Splitting Using Mixed Conducting Membranes, Proc. National Hydrogen Assoc. 14th Annual U.S. Hydrogen Meeting, Washington, DC, March 4-6, 2003.

Current Status of Mixed-Conducting Ceramic Membranes for Gas Separation Applications, presented at the Univ. of Houston, March 14, 2003.

Dense Cermet Membranes for Hydrogen Separation, presented at the 225th Amer. Chem. Soc. Natl. Mtg., Fuel Chemistry Div., New Orleans, March 23-27, 2003.

Hydrogen Production by Water Dissociation Using Mixed-Conducting Membranes, presented at 225th Amer. Chem. Soc. Natl. Mtg., Fuel Chemistry Div., New Orleans, March 23-27, 2003.

Current Status of Mixed-Conducting Ceramic Membranes for Gas Separation Applications, presented at the University of Illinois, Urbana-Champaign, April 24, 2003.

Hydrogen Production by Water Dissociation Using Oxygen-Permeable Cermet Membranes, presented at 105th Ann. Mtg. of Amer. Ceramic Soc., Nashville, April 27-30, 2003.

Preparation and Characterization of New Mixed Conducting Oxides $\text{Ba}(\text{Zr}_{0.8-x}\text{Pr}_x\text{Y}_{0.2})\text{O}_{2.9}$, presented at 105th Ann. Mtg. of Amer. Ceramic Soc., Nashville, April 27-30, 2003.

Metal/Ceramic Composites with High Hydrogen Permeability, U.S. Patent #6,569,226, May 27, 2003.

Current Status of Dense Cermet Membranes for Hydrogen Separation, presented at the 20th Annual Intl. Pittsburgh Coal Conf., Pittsburgh, Sept. 15-19, 2003; in Conf. Proc., S46, 187.PDF, 2003.

Current Status of Ceramic Membranes for Hydrogen Production and Separation Applications, presented at the U. of Alaska-Fairbanks, Sept. 24, 2003.

Hydrogen Production by Water Dissociation Using Mixed Conducting Membranes, presented at Second Information Exchange Meeting on Nuclear Production of Hydrogen, Argonne Natl. Lab., Oct. 2-3, 2003.

A Method to Remove Ammonia using a Proton-Conducting Membrane, U.S. Patent #6,630,116, Oct. 7, 2003.

- Numerical Modeling of Hydrogen Permeation in Chemical Potential Gradients, *Solid State Ionics*, 164, 107 (2003).
- Development of Dense Cermet Membranes for Hydrogen Separation, presented at the 204th Mtg. of the Electrochemical Soc., Orlando, Oct. 12-17, 2003.
- Hydrogen Permeation of Cermet Ba(Ce_{0.6}Zr_{0.2})Y_{0.2}O₃/Ni Membranes, presented at the 204th Mtg. of the Electrochemical Soc., Orlando, Oct. 12-17, 2003.
- Hydrogen Permeability of SrCe_{1-x}M_xO_{3-d} (x = 0.05, M = Eu, Sm), *Solid State Ionics*, 167, 99 (2004).
- Use of Mixed Conducting Membranes to Produce Hydrogen by Water Dissociation, *Intl. J. Hydrogen Energy*, 29, 291-296 (2004).
- Hydrogen Production by Water Dissociation using Mixed-Conducting Ceramic Membranes, *Proc. of National Hydrogen Assoc. 15th Annual U.S. Hydrogen Energy Conf.*, Los Angeles, CA, April 27-30, 2004.
- Mixed-Conducting Dense Ceramic Membranes for Hydrogen Production and Separation from Methane, presented at 15th World Hydrogen Energy Conf., Yokohama, Japan, June 27-July 2, 2004.
- Hydrogen Production from Water Using Mixed-Conducting Ceramic Membranes, presented at 15th World Hydrogen Energy Conf., Yokohama, Japan, June 27-July 2, 2004.
- Development of Dense Ceramic Membranes for Hydrogen Production and Separation, *Proc. of 8th Intl. Conf. on Inorganic Membranes*, eds., F. T. Akin and Y. S. Lin, Adams Press, Chicago, IL (2004), pp. 163-166.
- Development of Dense Cermet Membranes for Hydrogen Separation, presented at 21st Annual Intl. Pittsburgh Coal Conf., Osaka, Japan, Sept. 13-17, 2004.
- Hydrogen Permeation of Cermet [Ni-Ba(Ce_{0.6}Zr_{0.2})Y_{0.2}O_{3-δ}] Membranes, presented at the 206th Mtg. of the Electrochemical Soc., Honolulu, Oct. 3-8, 2004.
- Development of Dense Ceramic Membranes for Hydrogen Production and Separation, presented at American Soc. for Materials--Annual Materials Solution Conf., Columbus, OH, Oct. 18-21, 2004.
- Electrical and Hydrogen Transport Properties of SrCe_{0.8}Yb_{0.2}O_{3-δ}/Ni Cermet Membranes, presented at Fall Meeting of Materials Research Society, Boston, Nov. 29-Dec. 3, 2004.
- Preparation and Hydrogen Pumping Characteristics of BaCe_{0.8}Y_{0.2}O_{3-δ} Thin Film, presented at Fall Meeting of Materials Research Society, Boston, Nov. 29-Dec. 3, 2004.
- Hydrogen Permeability and Microstructure Effect of Mixed Protonic-Electronic Conducting Eu-Doped Strontium Cerate, *J. Mater. Sci.*, 40, 4061-4066 (2005).
- Defect Structure and Transport Properties of Ni-SrCeO_{3-δ} Cermet for Hydrogen Separation Membrane, *J. Electrochem. Soc.* 152(11), J125 (2005).
- Dense Cermet Membranes for Hydrogen Separation, presented at American Institute of Chemical Engineers (AIChE) Spring National Meeting, Atlanta, GA, April 10-14, 2005.

Hydrogen Separation Using Dense Cermet Membranes, presented at 30th Intl. Tech. Conf. on Coal Utilization and Fuel Systems, Clearwater, FL, April 17-21, 2005.

Electrical and Hydrogen Transport Properties of SrCe_{0.8}Yb_{0.2}O_{3-δ}/Ni Cermet Membranes, Mat. Res. Soc. Symp. Proc., 835, K3.2 (2005).

Preparation and Hydrogen Pumping Characteristics of BaCe_{0.8}Y_{0.2}O_{3-δ} Thin Film, Mat. Res. Soc. Symp. Proc., 835, K1.5 (2005).

Structure, Proton Incorporation and Transport Properties of Ceramic Proton Conductor Ba(Ce_{0.7}Zr_{0.2}Yb_{0.1})O_{3-d}, Mat. Res. Soc. Symp. Proc., 835, K1.4 (2005).

Development of Dense Ceramic Membranes for Hydrogen Separation, presented at 2005 DOE Annual Hydrogen Program Review, Washington, DC, May 23-25, 2005.

Membranes: The Good, The Bad, and The Ugly, presented to Hydrogen & Fuel Cell Tech. Prog. Office, DOE, Wash., DC, June 8, 2005.

Thin Film Preparation and Hydrogen Pumping Characteristics of BaCe_{0.8}Y_{0.2}O_{3-δ}, Solid State Ionics, 176, 1479-1484 (2005).

Hydrogen Production by Water Splitting Using Dense Thin-Film Cermet Membranes, presented at Fall Meeting Materials Research Society, Boston, Nov. 28-Dec. 2, 2005.

Hydrogen Permeation and Chemical Stability of Cermet [Ni-Ba(Zr_{0.8-x}Ce_xY_{0.2})O₃] Membranes, Electrochem. & Solid State Lett., 8(12), J35-J37 (2005).

Electrochemical Hydrogen Pumping Characteristics of BaCe_{0.8}Y_{0.2}O_{3-δ} Thin Film, presented at Electrochem. Soc. 2005 Fall Mtg., Los Angeles, Oct. 16-21, 2005.

Defect Structure and Transport Properties of Ni-SrCeO_{3-δ} Cermet for Hydrogen Separation Membrane, J. Electrochem. Soc., 152 (11), J125, 2005.

Review: Stress-Induced Diffusion and Cation Defect Chemistry Studies of Perovskites, invited paper published in "Defects & Diffusion in Ceramics – An Annual Retrospective VII: Defect & Diffusion Forum," Scitec Publication, London, UK (Oct. 2005), pp. 43-63.

Hydrogen Production by Water Dissociation Using Mixed Oxygen Ion-Electron Conducting Membranes, presented at Electrochem. Soc. 2005 Fall Mtg., Los Angeles, Oct. 16-21, 2005.

Hydrogen Permeation of Ceramic/Metal Composite Thin Films, presented at Electrochem. Soc. 2005 Fall Mtg., Los Angeles, Oct. 16-21, 2005.

Development of Dense Cermet Membranes for Hydrogen Separation, invited presentation at World Hydrogen Technologies Convention, Singapore, Oct. 3-6, 2005.

Mixed-Conducting Dense Ceramic Membranes for Air Separation and Natural Gas Conversion, J. Solid State Electrochem., 10, 617-624 (2006).

Hydrogen Separation by Dense Cermet Membranes, Fuel, 85(2), 150-155 (2006).

Hydrogen Production by Water Dissociation Using Mixed-Conducting Dense Ceramic Membranes, invited presentation at Amer. Chem. Soc. 231st Natl. Mtg., Atlanta, March 26-30, 2006.

Development of Dense Membranes for Hydrogen Production and Separation, Invited Talk at the 2nd Energy Center Hydrogen Initiative Symposium, Purdue University, West Lafayette, IN, April 12-13, 2007.

Development of Dense Cermet Membranes for Hydrogen Separation, presented at AIChE Spring Mtg., Orlando, FL, April 23-27, 2006.

Hydrogen Production from Methane Using Dense Oxygen and Hydrogen Transport Membranes, presented at 209th Electrochemical Soc. Mtg., Denver, May 7-12, 2006.

Development of Dense Hydrogen Transport Membranes, presented at the 31st International Technical Conference on Coal Utilization and Fuel Systems, Clearwater, FL, May 21-25, 2006.

Annealing Effect of Cermet Membranes on Hydrogen Permeability, Chem. Lett., 35(12), 1378-1379 (2006).

Mixed-conducting Membranes for Hydrogen Production and Separation, Invited presentation at 2006 MRS Fall Meeting, Boston, MA, Nov. 27 – Dec. 1, 2006.

Dense Cermet Membranes for Hydrogen Separation from Mixed Gas Streams, presented at 23rd Annual Intl. Pittsburgh Coal Conf., Pittsburgh, PA, Sept. 25-28, 2006.

Effect of Zr-Doping on the Chemical Stability and Hydrogen Permeation of the Ni-BaCe_{0.8}Y_{0.2}O_{3- δ} Mixed Protonic-Electronic Conductor, Chemistry of Materials, 18(19), 4647 (2006).

Composite Ni-Ba(Zr_{0.1}Ce_{0.7}Y_{0.2})O₃ Membrane for Hydrogen Separation, J. Power Sources, 159(2), 1291 (2006).

Dense Membranes for Hydrogen Separation and Purification, in "Materials for the Hydrogen Economy," CRC Press LLC, Boca Raton, FL, 2007.

Stability of Dense Cermet Membranes for Hydrogen Separation, presented at 211th Meeting of Electrochemical Society, Chicago, IL, May 6-10, 2007.

Development of Dense Membranes for Hydrogen Production from Coal, Invited Talk at 234th American Chemical Society National Meeting, Boston, MA; Aug. 19-23, 2007.

Chemical Stability of Hydrogen Transport Membranes, presented at the 24th Annual International Pittsburgh Coal Conference, Johannesburg, South Africa, Sept. 10-14, 2007.

Dense Membranes for Hydrogen Separation and Purification, "Materials for the Hydrogen Economy," CRC Press LLC, Boca Raton, FL (in press, 2008).

Development of Dense Membranes for Hydrogen Production and Purification, presented at the American Ceramic Society's Materials Innovations in an Emerging Hydrogen Economy, Cocoa Beach, FL, Feb. 24-26, 2008.

Status of Hydrogen Separation Membrane Development, presented at National Hydrogen Assoc. Annual Hydrogen Conf., Sacramento, CA, March 30 – April 4, 2008.

Development of Dense Membranes for Hydrogen Separation from Coal Gasification Streams, presented at joint AIChE/ACS Spring 2008 Meeting, New Orleans, LA, Apr. 6-10, 2008.

Development of Membranes for Purifying Hydrogen Produced by Coal Gasification and/or Methane Reforming, presented at the 25th Annual Intl. Pittsburgh Coal Conf., Pittsburgh, PA, Sept. 29-Oct. 2, 2008.

The Effect of Hydrogen Partial Pressure on UNiaxial Creep of 3Y-TZP/50 vol. % Pd Cermet Membranes, *Materials Science and Engineering B*, 150 (3), 145-150 (2008).

REFERENCES

1. U. Balachandran, Argonne National Laboratory Hydrogen Separation Membranes--Annual Report for FY 2006.
2. U. Balachandran, Hydrogen Separation Membranes--Annual Report for FY 2007, Argonne National Laboratory.
3. U. Balachandran, Hydrogen Separation Membranes--Annual Report for FY 2005, Argonne National Laboratory.
4. U. Balachandran, Hydrogen Separation Membranes--Quarterly Report for April-June 2007, Argonne National Laboratory.
5. U. Balachandran, Hydrogen Separation Membranes--Quarterly Report for October-December 2006, Argonne National Laboratory.
6. S. A. Koffler, J. B. Hudson, and G. S. Ansell, *Trans. Met. Soc. AIME*, 245, 1735 (1969).
7. U. Balachandran, Hydrogen Separation Membranes--Annual Report for FY 2003, Argonne National Laboratory.
8. J. T. Richardson, *Principles of Catalyst Development*, Plenum Press, New York, NY (1989).
9. U. Balachandran, Hydrogen Separation Membranes--Quarterly Report for April-June 2008, Argonne National Laboratory.
10. U. Balachandran, Hydrogen Separation Membranes--Quarterly Report for January-March 2008, Argonne National Laboratory.
11. U. Balachandran, Argonne National Laboratory Hydrogen Separation Membranes--Annual Report for FY 2000.
12. T. Matsui, M. Harada, M. Toba, and Y. Yoshimura, *Appl. Catal. A*, 293, 137-144 (2005).
13. H. Yasuda and Y. Yoshimura, *Catal. Lett.*, 46, 43-48 (1997).



Energy Systems Division

Argonne National Laboratory
9700 South Cass Avenue, Bldg. 212
Argonne, IL 60439-4838

www.anl.gov



U.S. DEPARTMENT OF
ENERGY

A U.S. Department of Energy laboratory
managed by UChicago Argonne, LLC